Spontaneous acoustic emission of a corrugated shock wave in the presence of a reflecting surface

J. G. Wouchuk and J. López Cavada
ETSI Industriales, Universidad de Castilla–La Mancha, 13071 Ciudad Real, Spain
(Received 9 January 2004; revised manuscript received 24 June 2004; published 11 October 2004)

An analytic model to study perturbation evolution in the space between a corrugated shock and a piston surface is presented. The conditions for stable oscillation patterns are obtained by looking at the poles of the exact Laplace transform. It is seen that besides the standard D'yakov-Kontorovich (DK) mode of oscillation, the shock surface can exhibit an additional finite set of discrete frequencies, due to the interaction with the piston which reflects sound waves from behind. The additional eigenmodes are excited when the shock is launched at $t=0^+$. The first eigenmode (the DK mode) is always present, if the Hugoniot curve has the correct slope in the *V-p* plane. However, the additional frequencies could be excited for strong enough shocks. The predictions of the model are verified for particular cases by studying a van der Waals gas, as in the work of Bates and Montgomery [Phys. Fluids **11**, 462 (1999); Phys. Rev. Lett. **84**, 1180 (2000)]. Only acoustic emission modes are considered.

DOI: 10.1103/PhysRevE.70.046303 PACS number(s): 47.20.−k, 47.40.−x, 52.57.−z

I. INTRODUCTION

The study of shock waves is a subject of great theoretical and practical importance in hydrodynamics and related fields. Extensive use has been and is still being made of shock waves to study the properties of gases, liquids, and solids at high pressures and temperatures for equation of state (EOS) measurements [1–3]. Subsidiary to these experiments we face the problem of shock front stability when subjected to corrugations of small amplitude. In fact, the growth or decay of the perturbations imposed at the surface of the shock is an issue of fundamental importance that has fascinated the scientific community during the last 50 years. We could find perturbed shock fronts in astrophysical phenomena [4], geophysical experiments [5], and inertial confinement fusion (ICF) implosions [6–9]. The hydrodynamic fluctuations generated by deformed shock waves could actually trigger deleterious hydrodynamic instabilities in ICF targets, namely, the Richtmyer-Meshkov (RM) and the Rayleigh-Taylor (RT) instabilities [9–19]. The first theoretical works that dealt with the stability properties of corrugated shock fronts are those of Roberts [20], D'yakov [21], and Kontorovich [22,23] The early work of Roberts studied the evolution of a corrugated shock wave that moved into an ideal gas. He showed that the initial ripple at the shock surface would eventually show damped oscillations as the shock moved away from the interface and the shock surface would regain the planar shape. The solution was analytical and made use of Laplace transforms of the fluid equations in the linear approximation. On the other hand, the works of D'yakov and Kontorovich studied the interaction of a planar shock front with sound waves that collided with the shock from either ahead or behind, and made an eigenmode analysis of the perturbations that develop at the corrugated front. They obtained explicit conditions for stability in terms of the shock front Mach number, density compression ratio, and the slope of the Rankine-Hugoniot curve at the final compression state. In particular, they derived an explicit criterion (from now on we call it the DK criterion) in order for the corrugations at the shock wave to show a stable oscillatory behavior as a function of time. That is, their result gives sufficient and necessary conditions for the shock front to oscillate with a characteristic frequency without damping, the so called spontaneous acoustic emission (SAE) and is expressed for a general equation of state. The same problems were later studied in detail by Erpenbeck [24], Fowles, and Swan [25–28]. Recently, the subject of shock stability has also seen a renewed interest as it can provide important insights into the dynamics of shock waves propagating in metals [29], diatomic gases [30,31], and in situations of astrophysical interest [32]. The problem of shock stability in ideal gases has been investigated again in a recent work by Robinet *et al.* [33]. All the previous works have emphasized the importance of the slope of the Hugoniot curve in order to study the stability properties of the shock wave. As usual, let us consider the quantity

$$h = \frac{p_1 - p_f}{V_1 - V_f}\left(\frac{dV}{dp}\right)_H. \tag{1}$$

The quantity V is the specific volume of the fluid. The subscript "f" refers to the final compressed state and the subscript "1" refers to the initial state of the fluid. The derivative is taken along the Hugoniot curve and calculated at the final compressed state. The work of D'yakov and Kontorovich showed that the condition for the emission of undamped sound waves from the shock surface is

$$h_c < h < 1 + 2M_f, \tag{2}$$

where M_f is the shock wave Mach number with respect to the compressed fluid, and h_c is defined by

$$h_c = \frac{1 - M_f^2(1 + \rho_f/\rho_1)}{1 - M_f^2(1 - \rho_f/\rho_1)}, \tag{3}$$

with ρ_f the density of the compressed fluid, and ρ_1 the initial density before shock compression. Ideal fluids do not satisfy the previous inequality and hence there is no possibility of observing acoustic emission in ideal gases. On the contrary, some other substances with nonideal equations of state may

satisfy the previous inequality in some domain of the space of physical parameters [1–7,21–31].

The usual approach to derive the above inequality consists in perturbing the shock surface and doing a normal mode analysis for the perturbations in the compressed fluid. All perturbed quantities behind the shock surface are assumed to depend on the spatial and temporal coordinates in the separable form [1]

$$\delta\phi(x,y,t) \equiv A \exp[i(k_x x' + k_y y' - \omega t)], \tag{4}$$

where $\delta\phi$ represents the linear perturbation of any fluid quantity ϕ. The coordinate x' is in the direction normal to the shock front where the positive x' axis points inside the compressed fluid. The coordinate y' is in the tangential direction. Equation (4) is proposed in a reference frame moving with the shock surface. The quantities k_x and k_y are the projections of the perturbation wave number along the coordinate axis and t is the time. The Rankine-Hugoniot conditions are linearized around the final state and a dispersion relation is obtained that enables us to calculate the frequency of the oscillations as a function of the wave number. Usually, far behind the shock (namely, the piston surface), all the perturbations are assumed to vanish [1,5,22,25,31] in order that the perturbation field be bounded in the whole space. Adopting this approximation, the usual DK stability criterion is obtained for the emission of undamped acoustic waves [1,5,22,25]. In the present work we relax this boundary condition far behind the shock. In fact, as is already known from the research done in the RM instability, the dependence of the perturbed quantities on the variables x and t may not be always written in the separable form as expressed in the previous Eq. (4). The reason is that one of the boundaries (either the shock front or the piston surface) is moving in time and therefore the domain of integration is not square as in the x,t space. The consequence is that we cannot use separation of variables in the x,y,t space to integrate the wave equation. As a matter of fact, the exact solution to the wave equation in the space between the piston and the shock is written as [8,10,33–36]

$$\delta\phi(x,y,t) = f_1((c_f t - x)/(c_f t + x)) f_2(k^2(c_f t - x) \times (c_f + x))\cos ky, \tag{5}$$

where f_1 and f_2 are suitable functions that must be determined from the boundary and initial conditions at both the shock front and the piston surface [10,12]. The quantity k is the piston perturbation wave number, which is equal to $2\pi/\lambda$, and λ is the perturbation wavelength. In principle, the previous solution would not look like Eq. (4) in the general case. We must stress the fact that, even if the approximate form adopted in Eq. (4) is used, the DK criterion [Eqs. (2) and (3)] is, however, correct. The reason is that the DK mode of oscillation does not actually interact with the shock after reflection at the piston surface. That is, when Eq. (2) is satisfied, the shock emits sound waves at the DK frequency, and those waves would reach the piston and reflect there. However, the angle of reflection would be such that the reflected sound wave would never catch the shock, because the projection of the velocity of the sound wave along the direction normal to the shock will always be less than the shock speed itself [23]. This means that the DK shock mode of oscillation does not couple piston and shock. Therefore, as far as the evolution of this mode of oscillation is concerned, the exact boundary condition at the piston is irrelevant. Actually, the corrugated piston is only necessary (at $t=0^+$) in order to excite the DK oscillation mode. Immediately afterward, any sound wave emitted with frequency and wave vector corresponding to the DK mode would be reflected some time later, without hitting the shock ever again. This fact explains the accuracy of all the previous work in getting the DK mode while "forgetting" the piston surface. However, this approximate boundary condition at the piston surface does not allow for the mathematical solution to display the additional modes of oscillation of the shock front that can be excited at higher shock intensities. We know that, depending on the boundary condition we require at the piston surface, the structure of the perturbation field behind the front could be different [9,10,37,42]. It will be seen later that, in addition to the expected DK mode of oscillation, additional modes for acoustic emission could appear and the shock front ripple would oscillate as a result of the superposition of all those modes. In order for the shock to oscillate with these additional eigenfrequencies, the standard DK criterion [Eq. (2)] needs to be modified and the lower bound would be another function of the shock compression ratio and the shock Mach number. This phenomenon occurs for relatively strong shocks. Similar conclusions can be obtained for the perturbations at the piston. We could find zones in the space of physical parameters in which the pressure perturbations at the piston also show stable oscillations, as a result of constructive interference of the wave pattern that fills the space behind the shock.

Up to now, the perturbation problem has always been solved by considering the evolution of a single isolated shock. Due to the inherent mathematical difficulties of including a reflecting piston in the space behind the shock, the possible generalization of Eq. (2) in this case has never been considered for an arbitrary EOS. It is usually assumed that piston and shock separate quickly from each other, and therefore any asymptotic solution that appears for sufficiently large times will not feel the piston causal influence. However, as will be shown in the rest of the work, stable acoustic emission modes (either the classical DK mode, or the ones found in this work) are excited at the shock surface since $t=0^+$. That is, when the shock and piston are still very near each other. As a matter of fact, the perturbation at the shock can always be thought of as a superposition of the form $\delta p_{SAE}(t) + \delta p_{dec}(t)$, valid in the whole interval $0+ \leqslant t < \infty$. The function $\delta p_{SAE}(t)$ is the possible oscillating contribution from the acoustic emission modes, and $\delta p_{dec}(t)$ is that part of the solution that decays in time. In fact for an ideal gas, it is always $\delta p_{SAE} \equiv 0$, and we only get the well known decaying oscillations, which behave like $\delta p_{dec}(t) \sim t^{-3/2}$ for large times [10]. On the contrary, for another EOS, we could see a nonzero stable contribution $\delta p_{SAE}(t) \neq 0$. These stable perturbations could be the result of oscillations with only one frequency (as in the standard DK situation) or even with more frequencies (due to the effect of the right facing sound waves

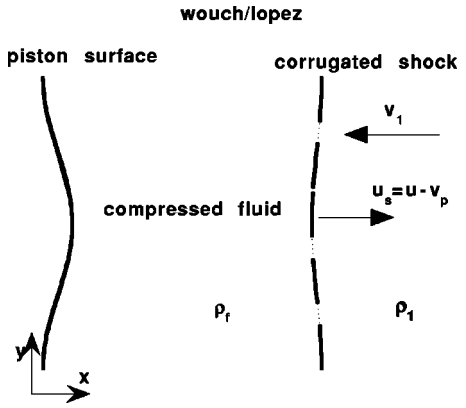

FIG. 1. Corrugated shock front moving ahead of a corrugated rigid piston. The piston has a transverse corrugation of amplitude ψ_0 and wavelength λ. For explanation of the symbols, see the text of the paper.

impinging on the shock and assuming that the Hugoniot curve has the correct slope in the pressure-volume plane, and the shock intensity is high enough). It will be shown that these additional stable modes can be excited *only* if we include the shock-piston interaction in the formulation of the problem. Of course, if the Hugoniot curve has not an adequate slope for the additional set of waves to appear, only the standard DK waves will show up [when Eq. (2) holds]. It is therefore clear that the standard DK criterion should be generalized to include the effect on the shock evolution of the sound waves reflected at the piston. The results obtained here are based on exact and rigorous linear theory, as already used to solve the linear perturbation problem of the RM instability [37,38].

This work is organized as follows. In Sec. II the exact solution in the space of physical coordinates x,y,t is obtained. The Laplace transform of the pressure perturbations is also calculated as a solution of a functional equation. The limits of validity of the solution are discussed. The stability properties of the flow are examined in Sec. III by looking for the poles of the Laplace function. Only the specific case of spontaneous acoustic emission is considered. The additional spectrum for the shock front oscillations is derived analytically. In Sec. IV the results of the preceding sections are calculated in analytical form and used to study a real gas equation of state as in Refs. [6,7]. The frequencies and mode amplitudes are compared with the results of the linear series expansion deduced in Sec. II. A qualitative discussion of the results and a comparison with the findings of previous works is given in Sec. V. A brief summary is presented in Sec. VI.

II. PRESSURE PERTURBATION FIELD BETWEEN THE PISTON AND THE SHOCK FRONT

A. Wave equation

In Fig. 1 we show the geometry of the shock and the piston surface. In the laboratory frame of reference, the piston starts suddenly to move at $t=0$ with velocity $v_p\hat{x}$. As the surface of the piston is corrugated, a perturbed shock front will be launched at $t=0^+$ that moves to the right with velocity $u\hat{x}$. It is convenient to study the hydrodynamic perturbations in a system in which the piston surface is at rest. From now on, we will work in the piston reference frame. Therefore, the shock moves to the right with velocity $u_s\hat{x}=(u-v_p)\hat{x}$ compressing the fluid from its initial density ρ_1 to its final value ρ_f. The fluid has a velocity $-v_1\hat{x}$ ahead of the shock and comes to rest after crossing the shock front. We consider an arbitrary EOS for the fluid and do not restrict the model to ideal gases. The sound speed of the compressed fluid is c_f. The piston wall has a corrugation of wavelength λ and amplitude ψ_0. We assume linear perturbations, so that $\psi_0 \ll \lambda$. As the shock moves away from the piston, the amplitude of its ripple will change in time. Depending on the properties of the fluid being compressed, the ripple amplitude could decay, show stable oscillations or actually grow. We will concentrate on the conditions that enable the shock front ripple to oscillate with a characteristic frequency.

We linearize the fluid equations, assuming that the dependence on the y coordinate scales like $\cos ky$ for the pressure perturbations $\delta p(x,y,t)$. In order to solve the equations by separation of variables, we use the following coordinate transformation, as suggested by Zaidel' [34–37]: $r\cosh\theta = kc_f t$, $r\sinh\theta = kx$. The shock wave coordinate is defined by $\beta_s = \tanh\theta_s = u_s/c_f < 1$. The piston surface is defined by $\theta_p = 0$. After some algebra, the fluid equations can then be combined into a wave equation for the dimensionless pressure fluctuations $\delta\hat{p}$, in the new coordinates [37,38]

$$r\frac{\partial^2\delta\hat{p}}{\partial r^2} + \frac{\partial\delta\hat{p}}{\partial r} + r\delta\hat{p} = \frac{\partial}{\partial\theta}\left(\frac{1}{r}\frac{\partial\delta\hat{p}}{\partial\theta}\right), \tag{6}$$

where $\delta\hat{p}$ is defined by $\delta p(x,y,t) = \rho_f c_f^2 \delta\hat{p}(x,t)\cos ky$. The equation above can be solved in two different ways. The simplest one consists in solving it in the physical space r,θ by means of series of Bessel functions. The coefficients of the expansion are determined from the boundary conditions at the shock and at the piston, in much the same way as has been done to study the RM instability [36,39]. The other approach consists in Laplace transforming the wave equation and the boundary conditions. In this way, a functional equation for the Laplace transform of the pressure fluctuations at the shock front is readily obtained. As for the series expansion solution, it is easy to see that the following function is the most general solution of the wave equation that satisfies $\delta p(t=0^+)=0$ [8,34–36,39]:

$$\delta\hat{p} = \sum_\nu D_\nu(\theta) J_\nu(r). \tag{7}$$

The functions J_ν are the ordinary Bessel functions [40]. The coefficients D_ν are functions of the coordinate θ and must be determined with the boundary conditions. As already discussed in Refs. [36–38] they are given by $D_\nu = \pi_\nu \cosh\nu\theta$, where π_ν have to be determined from the shock boundary conditions.

B. Boundary conditions at the shock front

At the initial instant of time, the shape of the shock front will reproduce the corrugation at the piston wall. Therefore,

let $\psi_s(t)\cos ky$ be the shock front ripple. Its amplitude $\psi_s(t)$ is a function of time and its initial value is ψ_0. For the sake of simplicity in the notation, let us define the dimensionless velocity perturbations δu and δv by $\delta v_x(x,y,t) = \delta u(x,t)\cos ky$, $\delta v_y(x,y,t) = \delta v(x,t)\sin ky$ and the dimensionless density perturbation $\delta\hat{\rho}$ by $\delta\rho(x,y,t) = \delta\hat{\rho}(x,t)\cos ky$. After some algebra with the linearized Rankine-Hugoniot equations, the boundary conditions at the shock front can be combined into a single equation that couples both the shock front ripple and the pressure perturbation, in the r,θ coordinates [12,37,39]:

$$W_1\left(\frac{\partial\delta\hat{p}}{\partial r}\right)_{\theta_s} = \frac{W_2}{r}\left(\frac{\partial\delta\hat{p}}{\partial\theta}\right)_{\theta_s} + \frac{E}{\cosh\theta_s}\xi_s, \tag{8}$$

where $\xi_s = k\psi_s$, and the equation for ξ_s is

$$\frac{\partial\xi_s}{\partial r} = \frac{1}{2\beta_s}\frac{(h+1)\cosh\theta_s}{1-\rho_1/\rho_f}(\delta\hat{p})_{\theta_s}. \tag{9}$$

The constants $W_{1,2}$ and E are

$$W_1 = -\frac{(1-\beta_s^2)(h-1)}{1+2\beta_s^2-h},\ W_2 = -\frac{2\beta_s(1-\beta_s^2)}{1+2\beta_s^2-h},\ E = -\frac{2\beta_s^2}{1+2\beta_s^2-h}\frac{v_1}{c_f}. \tag{10}$$

Equations (8) and (9) are the boundary conditions at the shock front. To find the coefficients of the series expansion [Eq. (7)], it is better to work with the Laplace transform of the perturbations at the shock front [39]. We previously define the Laplace transform of any perturbed quantity $\delta\phi(r,\theta)$ (from now on, Laplace transforms are indicated with capital letters) as

$$\delta\Phi(s,\theta) = \int_0^\infty dr\, e^{-sr}\delta\phi(r,\theta), \tag{11}$$

and change to the new variable q defined by $s=\sinh q$, as suggested by Zaidel' [33]. After some algebra, we find the coefficients π_1 and π_3 [39]:

$$\pi_1 = 2E\xi_0, \tag{12}$$

$$\pi_3 = \frac{2(W_1+2EA)\cosh^2\theta_s+1}{(W_1-W_2\tanh 3\theta_s)\cosh\theta_s\cosh 3\theta_s}\pi_1. \tag{13}$$

The other coefficients are found after solving the recurrence equation

$$\pi_{2n+1} = \frac{2(W_1+2EA)\cosh(2n-1)\theta_s}{[W_1-W_2\tanh(2n+1)\theta_s]\cosh(2n+1)\theta_s}\pi_{2n-1} - \frac{[W_1+W_2\tanh(2n-3)\theta_s]\cosh(2n-3)\theta_s}{[W_1-W_2\tanh(2n+1)\theta_s]\cosh(2n+1)\theta_s}\pi_{2n-3}, \tag{14}$$

where $A = 1/(2\beta_s)(h+1)/[1-(\rho_1/\rho_f)]$.

C. Functional equation for the Laplace transform of the pressure perturbations

After some algebra, and using the fact that our piston is a rigid wall, the Laplace transforms of the pressure perturbations at the shock can be seen to satisfy the functional equation [37]

$$\delta P_s(q) = \lambda_1(q) + \lambda_2(q)\,\delta P_s(q+2\theta_s), \tag{15}$$

where the functions $\lambda_{1,2}$ are given by

$$\lambda_1(q) = \frac{\alpha_2(q)+\alpha_2(q+2\theta_s)}{\cosh q-\alpha_1(q)},\qquad \lambda_2(q) = \frac{\cosh(q+2\theta_s)+\alpha_1(q+2\theta_s)}{\cosh q-\alpha_1(q)}. \tag{16}$$

The auxiliary functions $\alpha_{1,2}$ are

$$\alpha_1(q) = \alpha_{10}\sinh q + \frac{\alpha_{11}}{\sinh q},\ \alpha_2(q) = -\delta v_0\frac{\sinh\theta_s}{\sinh q}, \tag{17}$$

where the important parameters α_{10} and α_{11} are given by

$$\alpha_{10} = \frac{h-1}{2\beta_s},\ \alpha_{11} = -\frac{\beta_s}{2}\frac{h+1}{1-\beta_s^2}\frac{\rho_f}{\rho_1}, \tag{18}$$

and δv_0 is the initial lateral fluid velocity in the space between the shock and the piston (at $t=0^+$), given by $\delta v_0 = v_1 k\psi_0$. Equation (15) is an inhomogeneous linear functional equation of the first order [42,43]. The most general solution to it is the sum of a solution to the homogeneous equation plus a particular solution [34,42,43]. In this case, it is straightforward to find a particular solution. It is the result of an iterative sequence [37,42,43]

$$\delta P_s(q) = \lambda_1(q) + \sum_{j=1}^{\infty}\lambda_1(q+2j\theta_s)\prod_{n=0}^{j-1}\lambda_2(q+2n\theta_s). \tag{19}$$

Regarding the homogeneous solution [34,42,43], it is clear that it satisfies an equation of the form $\delta P_h(q+2\theta_s) = \delta P_h(q)/\lambda_2(q)$. As δP_s is a Laplace transform, it is clear that it should vanish when $\mathrm{Re}\,q\to\infty$. This will happen only when $|\lambda_2|>1$. This last condition is equivalent to asking for $h>1-2\beta_s^2$. Therefore, if h is bounded from below as in the last equation, the solution to the homogeneous equation should be added in Eq. (19). If, on the contrary, $h<1-2\beta_s^2$, the solution to the homogeneous equation is divergent and must be excluded from the general solution. In this work we will only study situations in which $h<1-2\beta_s^2$. Therefore, we take Eq. (19) as the complete and *exact* solution to the two-dimensional (2D) perturbation problem of a shock traveling into an undisturbed fluid driven by a reflecting piston. The cases that satisfy $h>1-2\beta_s^2$ are left for future research.

III. SPONTANEOUS ACOUSTIC EMISSION

A. Poles of the pressure function at the shock front

1. Standard DK mode of oscillation

As can be seen from the definitions of $\lambda_{1,2}$ [Eqs. (16)], the term $[\cosh q-\alpha_1(q)]$ is a common denominator to all the

terms in the right hand side of Eq. (19). Therefore, its poles give the information about the stably oscillating part of the solution in the x, t space. We remember that we are looking for the zeros which are pure imaginary numbers. It is noted that the commented factor can also be written as $1/[\sqrt{s^2+1}-\alpha_1(s)]$ in terms of the Laplace variable s. Therefore, we keep in mind that we must work with the positive determination of the square root. Let us make the variable change

$$s = \frac{1}{2}\left(e^{\alpha+i\beta} - \frac{1}{e^{\alpha+i\beta}}\right) \tag{20}$$

in terms of some new auxiliary variables α and β. If we are looking only for purely imaginary solutions in the variable s, then it is immediate to see that $\beta=\pm i\pi/2$. Then, $s=\pm(i/2)(e^{\alpha}+e^{-\alpha})$ and $\sqrt{s^2+1}=\pm(i/2)(e^{\alpha}-e^{-\alpha})$. In order to deal only with the positive determination of the square root, we must require $\alpha>0$. Then, our equation looks like

$$\frac{1}{2}\left(e^{\alpha} - \frac{1}{e^{\alpha}}\right) = \frac{\alpha_{10}}{2}\left(e^{\alpha} + \frac{1}{e^{\alpha}}\right) - \frac{2\alpha_{11}}{e^{\alpha}+1/e^{\alpha}}, \tag{21}$$

or

$$\sqrt{b^2-1} = \alpha_{10}\, b - \frac{\alpha_{11}}{b}, \tag{22}$$

where $b=(e^{\alpha}+e^{-\alpha})/2>1$. The last equation has a solution depending on the values of α_{10} and α_{11}. Let us first assume that both α_{10} and α_{11} are negative numbers. This is equivalent to saying that the D'yakov-Kontorovich parameter defined in Eq. (1) satisfies simultaneously: $h<1$ and $h>-1$ [see Eqs. (18)]. If we want to have SAE under these conditions, the function defined by the left hand side of Eq. (22) must intersect the right hand side at some value of b. Let the auxiliary function f be defined by $f(b)=\alpha_{10}\, b-(\alpha_{11}/b)$. Then, according to Fig. 2(a), a solution is possible only if $f(b=1)\geqslant 0$. According to Eqs. (18) this is equivalent, after some algebra, to requiring that $h_c<h$, with h_c the parameter defined in Eq. (3). It is easy to prove that $h_c>-1$ does always hold. Otherwise, we would obtain $\beta_s>1$ which is not possible for a compressive shock [1,2,26,27]. That is, for this special case, the condition for SAE is

$$h_c < h < 1. \tag{23}$$

The next case is that in which $\alpha_{10}>0$. We must distinguish between $0<\alpha_{10}<1$ and $\alpha_{10}>1$. In the first case, it must be that $1<h<1+2\beta_s$ which implies necessarily that $\alpha_{11}<0$ [according to Eqs. (18)]. This situation is shown in Fig. 2(b), and there is one possible solution again, if $f(b=1)\geqslant 0$, which implies $h_c<h$. If $\alpha_{10}>1$ it is clear from the figure that there is no intersection for the curves, and hence no possibility of SAE. If $\alpha_{11}>0$, we have $h<-1$, which makes $\alpha_{10}<0$. This situation is shown in Fig. 2(c) and it is clear that there is no possibility of intersection between the curves drawn there. That is, there is no acoustic emission for $h<-1$. If both α_{10} and α_{11} are positive numbers, we should simultaneously have $h>1$ and $h<-1$, which is impossible. Then, regarding the first shock eigenmode, we have arrived at the well known condition for acoustic emission summarized in Eq. (2). However, it is noted that the inequality $h_c<h<1+2\beta_s$ is actually

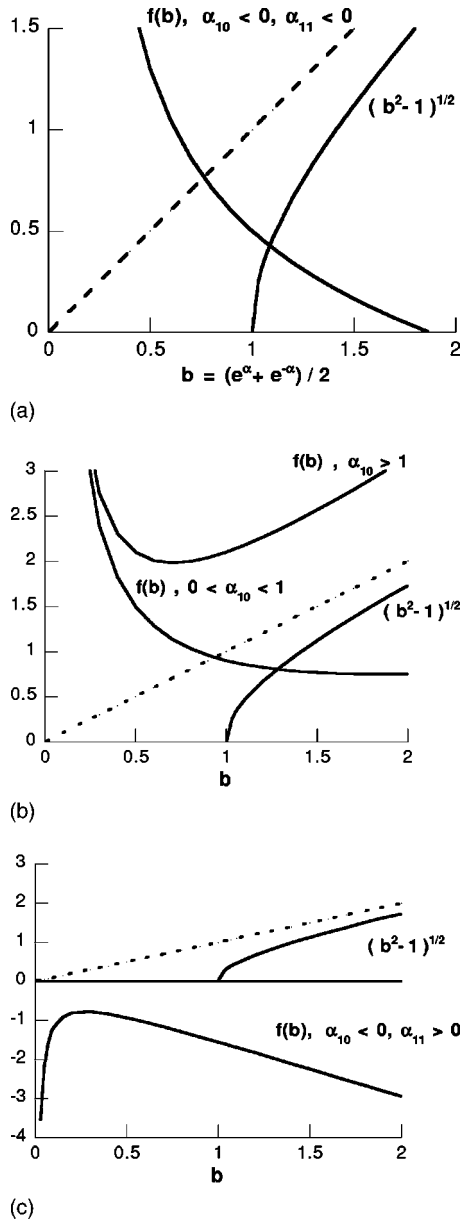

FIG. 2. (a) Conditions for the existence of an imaginary complex pole for δP_s. The curves drawn correspond to the case $\alpha_{10}<0$ and $\alpha_{11}<0$. For explanation of the symbols, see the text of the paper. (b) Same as (a), but the curves drawn here correspond to the case $0<\alpha_{10}<1$ and $\alpha_{11}<0$. For explanation of the symbols, see the text of the paper. (c) Same as (a), but the curves drawn here correspond to the case $\alpha_{10}<0$ and $\alpha_{11}>0$. For explanation of the symbols, see the text of the paper.

the union of two disjoint intervals. The first segment $[h_c<h<1]$ corresponds to situations that have $\alpha_{10}<0$, and the second segment $[1<h<1+2\beta_s]$ to situations in which $0<\alpha_{10}<1$. At least for the van der Waals gas cases studied in Sec. IV, only the first segment is always realized. We do not know if there is any Hugoniot curve that can realize both situations. Anyway, the common way of summarizing the standard criterion for SAE is to write the general Eq. (2) which results from the union of these two disjoint intervals. In addition, we recall that we do not include the solution to

the homogeneous functional equation, which makes our approach valid only in the range $h_c < h < 1-2\beta_s^2$. For situations in which $h > 1-2\beta_s^2$ the solution to the homogeneous equation could add additional modes of oscillation in addition to the modes found here. These cases will be studied in future work. Finally, before finishing this section, we solve Eq. (21) in order to get the frequency of the oscillation mode. It is not difficult to get a second order polynomic equation for the quantity $e^{2\alpha}$. We obtain, after some algebra,

$$T_0 \equiv e^{2\alpha_0} = \frac{\alpha_{10} - 2\alpha_{11} + \sqrt{1 + 4\alpha_{11}(\alpha_{11} - \alpha_{10})}}{1 - \alpha_{10}}, \quad (24)$$

where only the positive solution for α has been kept, that is, $T_0 > 1$. Then, the only two imaginary poles are $\pm i s_0$, where

$$s_0 = \frac{1}{2}\left(\sqrt{T_0} + \frac{1}{\sqrt{T_0}}\right). \quad (25)$$

Regarding the poles $\pm i s_0$, they correspond to the mode predicted by the DK criterion [1,3,5–7,21–33]. However, we also have additonal denominators which show a shift in the q variable. For example, the factor $1/[\cosh(q+2\theta_s) - \alpha_1(q+2\theta_s)]$ appears from the second term on, and factors of the form $1/[\cosh(q+4\theta_s) - \alpha_1(q+4\theta_s)]$ appear since the third term, and so on. Physically speaking, for very weak shocks, the first term $\lambda_1(q)$ would be more than enough to describe the perturbation field in the whole space with negligible error. That is, the additional terms, which are the functions λ_1 and λ_2 evaluated at values of q shifted by multiples of $2\theta_s$, become negligible and can be safely ignored. Thus, there are no additional poles besides $\pm i s_0$ for weak shocks. However, as the shock intensity increases, the shifted functions inside the solution δP_s become as important as the first nonshifted $\lambda_1(q)$ function. This is because, as the shock wave intensity increases, the downstream shock Mach number (β_s) decreases, and the interaction with the piston becomes more important. This fact is reflected by the parameter θ_s inside the argument of the $\lambda_{1,2}$ functions, which arise due to the Doppler shift after reflection of the sound waves coming from the piston on to the shock surface. The parameter θ_s is a monotonically decreasing function of the Mach number. For very weak shocks, the terms like $\lambda_{1,2}(q+2n\theta_s)$ with $n \geqslant 1$ are negligibly small and do not count in the perturbation evolution. For strong shocks, the influence of the (almost normal incidence) sound wave reverberations between the piston and the shock becomes more important. This behavior is a consequence of the fact that both the piston and the shock front "speak" to each other for a longer time for stronger shocks. For weaker shocks, this interaction can be neglected. Therefore, there is the possibility to excite additional modes at higher shock Mach numbers.

2. Additional modes of oscillation at the corrugated shock front

Let us consider for simplicity the lowest shift in the additional factors that compose δP_s, that is, terms of the form $1/[\cosh(q+2\theta_s) - \alpha_1(q+2\theta_s)]$. We are looking for poles of this term which are purely imaginary complex numbers. We will essentially follow the same technique as has been used in the previous section and make use of Eq. (20). After some straightforward algebra, and keeping in mind that we require $\alpha > 0$ and $\beta = \pm i\pi/2$, we get

$$b\cosh 2\theta_s + \sqrt{b^2-1}\sinh 2\theta_s = \alpha_{10}[b\cosh 2\theta_s + \sqrt{b^2-1}\sinh 2\theta_s] - \frac{\alpha_{11}}{[b\cosh 2\theta_s + \sqrt{b^2-1}\sinh 2\theta_s]}, \quad (26)$$

where $b = (e^{\alpha} + e^{-\alpha})$. Let us set

$$g(b) = \alpha_{10}[b\cosh 2\theta_s + \sqrt{b^2-1}\sinh 2\theta_s] - \frac{\alpha_{11}}{[b\cosh 2\theta_s + \sqrt{b^2-1}\sinh 2\theta_s]}. \quad (27)$$

The minimum possible value of b is $b=1$. Therefore, there will be a solution if $g(b=1)$ is greater than or equal to the left hand side of Eq. (27). that is, if the following inequality is satisfied:

$$\alpha_{11} \leqslant \alpha_{10}\cosh^2 2\theta_s - \sinh 2\theta_s \cosh 2\theta_s. \quad (28)$$

This condition can be rewritten in terms of the DK parameter h, and we get $h_{c2} < h$ where the parameter h_{c2} is given by

$$h_{c2} = \frac{1 - \beta_s^2(1 + \rho_f/\rho_1) + (1-\beta_s^2)[\sinh^2 2\theta_s + 2\beta_s \sinh 2\theta_s \cosh 2\theta_s]}{1 - \beta_s^2(1 - \rho_f/\rho_1) + (1-\beta_s^2)\sinh^2 2\theta_s}. \quad (29)$$

It can be seen that it is always $h_c < h_{c2}$. This means that the condition for the existence of the poles $\pm i s_0$ is also satisfied, which implies that the additional pole coexists with the DK mode. It is noted that a second pole would exist above a certain minimum Mach number. The same type of calculation can be done for all the factors of the form $1/[\cosh(q+2n\theta_s) - \alpha_1(q+2n\theta_s)]$ and the conditions needed in order to have a $(2n)$th order pole can be sought. The modifications to the previous equations are straightforward and we get

$$h_c < h_{c2} < h_{c4} < \cdots < h_{c2n} < h < 1 - 2\beta_s^2. \quad (30)$$

The quantity h_{c2n} is indexed according to the "number of shifts $2n\theta_s$" in the variable q that gave rise to the corresponding pole. Clearly, it is $h_c = h_{c0}$. For a given shock and EOS,

the DK parameter h could fall anywhere inside the subintervals defined in the above equation. Whichever is the actual subinterval, the standard DK mode will always be present [admitting that Eq. (23) holds]. The reason is that this mode is actually independent of the boundary condition at the piston, as will be discussed in Sec. V. Only the additional spectrum of modes depends on the existence of a left boundary that reflects the sound waves emitted by the shock. The boundary is only necessary to excite them at $t=0^+$, because of succesful reflection of sound waves at the piston and their subsequent interaction with the shock, as will be discussed in Sec. V.

Let us finish this paragraph by giving the expression for the imaginary poles that form the rest of the spectrum of the corrugated shock wave. To do it, we go back to Eq. (28), and note that it can be easily transformed into a polynomic equation of second degree in $e^{2\alpha}$, as before. After some algebraic manipulation, we can see that

$$T_2 \equiv e^{2\alpha_2} = T_0 e^{-4\theta_s} = \left[\frac{\alpha_{10} - 2\alpha_{11} + \sqrt{1 + 4\alpha_{11}(\alpha_{11} - \alpha_{10})}}{1 - \alpha_{10}} \right] e^{-4\theta_s}, \quad (31)$$

which can be easily generalized for the higher order poles as

$$T_{2n} \equiv e^{2\alpha_{2n}} = T_0 e^{-2n\theta_s} = \left[\frac{\alpha_{10} - 2\alpha_{11} + \sqrt{1 + 4\alpha_{11}(\alpha_{11} - \alpha_{10})}}{1 - \alpha_{10}} \right] e^{-2n\theta_s}. \quad (32)$$

Accordingly, the only two second poles are given by $\pm i s_2$, where s_2 is

$$s_2 = \frac{1}{2}\left(\sqrt{T_2} + \frac{1}{\sqrt{T_2}} \right), \quad (33)$$

and the general $(2n)$th order poles are $\pm i s_{2n}$, where

$$s_{2n} = \frac{1}{2}\left(\sqrt{T_{2n}} + \frac{1}{\sqrt{T_{2n}}} \right). \quad (34)$$

In Sec. IV we will show situations in which at least s_0 and s_2 are excited simultaneously for a real gas. Having calculated the poles and given the conditions for their existence, there remains the question of knowing how many additional eigenfrequencies are possible. The condition that $\alpha > 0$ implies that $|T_{2n}| > 1$. This means that the number n in Eqs. (32) and (34) is bounded from above. In other words the shock can be excited, at most, with a finite number of eigenfrequencies. The exact number depends on the EOS of the fluid. It can be given by taking the logarithm of Eq. (32):

$$(\text{number of poles at the shock}) \equiv n \leqslant \frac{\ln T_0}{2\theta_s}. \quad (35)$$

It is easy to see that the same analysis can be done for any surface at which the self-similar variable θ is constant (with $0 \leqslant \theta \leqslant \theta_s$). We will do it for the piston surface, which has $\theta = 0$, in the next subsection.

B. Poles of the pressure perturbation at the piston surface

We deduce here the functional equation satisfied by the piston pressure perturbations $\delta P_i(q)$. After some algebra, we get [37]

$$\delta P_i(q) = \chi_1(q) + \chi_2(q)\,\delta P_i(q + 2\theta_s), \quad (36)$$

where the functions χ_1 and χ_2 are given by

$$\chi_1(q) = \frac{2\alpha_2(q + \theta_s)}{\cosh(q + \theta_s) - \alpha_1(q + \theta_s)} \frac{\cosh(q + \theta_s)}{\cosh q},$$

$$\chi_2(q) = \frac{\cosh(q + \theta_s) + \alpha_1(q + \theta_s)}{\cosh(q + \theta_s) - \alpha_1(q + \theta_s)} \frac{\cosh(q + 2\theta_s)}{\cosh q}. \quad (37)$$

We can get a particular solution, in the same way as was done in Eq. (19). We just need to replace λ by χ. Regarding the validity of retaining only the particular solution, it is easy to see that this is licit to do only when $h < 1 - 2\beta_s^3$. This last inequality is satisfied assuming that $h < 1 - 2\beta_s^2$, because $\beta_s < 1$. Concerning the poles of δP_i the situation is essentially the same. Indeed, the poles are given by $\pm i s_{2n+1}$, where

$$s_{2n+1} = \frac{1}{2}\left(\sqrt{T_{2n+1}} + \frac{1}{\sqrt{T_{2n+1}}} \right), \quad (38)$$

where T_{2n+1} is calculated with

$$T_{2n+1} \equiv e^{2\alpha_{2n+1}} = T_0 e^{-2(2n+1)\theta_s}. \quad (39)$$

Obviously, the first pole at the piston appears at a high enough Mach number, such that a condition analogous to Eq. (27) is satisfied:

$$\alpha_{11} < \alpha_{10} \cosh^2 \theta_s - \sinh \theta_s \cosh \theta_s, \quad (40)$$

which can be, in turn, rewritten in terms of the DK parameter:

$$h_{c1} < h. \quad (41)$$

In general, for high enough shock Mach numbers we could define a $(2n+1)$th order pole, such that the condition for its existence is $h_{c(2n+1)} < h$ where $h_{c(2n+1)}$ is given by

$$h_{c(2n+1)} = \frac{1-\beta_s^2(1+\rho_f/\rho_1)+(1-\beta_s^2)[\sinh^2(2n+1)\theta_s+\beta_s \sinh 2(2n+1)\theta_s]}{1-\beta_s^2(1-\rho_f/\rho_1)+(1-\beta_s^2)\sinh^2 2n\theta_s}. \tag{42}$$

According to these results, the situation here does not seem to be very different from the oscillations found at the shock. To sum up the results of this section, in the general case, it would be possible to obtain a nested set of subintervals of the form

$$h_c < h_{c1} < h_{c2} < \cdots < h_{c(2n)} < h_{c(2n+1)} < h < 1-2\beta_s^2, \tag{43}$$

with n given by the upper bound of Eq. (35). The situation indicated in Eq. (43) would correspond to the simultaneous excitation of eigenmodes at the shock front and at the piston surface. The pressure oscillations at the piston would be further modulated by the natural frequency kc_f of the sound waves traveling in the resting fluid.

IV. SPONTANEOUS ACOUSTIC EMISSION AT A SHOCK FRONT MOVING INTO A VAN DER WAALS FLUID

A. Zero-order flow magnitudes

The model developed in the previous section is valid for any arbitrary EOS assuming that the fluid is inviscid. For an ideal gas equation of state, the inequalities displayed in Eq. (2) or Eq. (23) for the DK mode, or the more general inequality Eq. (43) would never be realized. This is a well known result: a corrugated shock moving in a homogeneous ideal gas is superstable [41,45] in the sense that any perturbation imposed on its surface would attenuate and the shock regains the planar shape. The situation is quantitatively different for a nonideal EOS. The simplest case to study is that of a real gas with a van der Waals EOS [2,6,7]. We use it here, as it provides us with a simple background flow on which the results deduced before can be shown. As is already known, the phenomena of acoustic emission are excited far from the ideal gas zone. That is, near the gas-liquid transformation curve in the V-p plane, where the nonideal characteristics of the gas are important. The dimensional equation of state is given by [2,7]

$$\left(p+\frac{a}{V^2}\right)(V-b) = Nk_BT, \tag{44}$$

where N is the number of molecules per unit mass, k_B is the Boltzmann's constant, and T is the temperature. The parameters a and b are specific to the gas and roughly speaking they take into account the finite volume of the molecules and the interaction among them. The thermodynamic variables of the critical point (V_{cr}, p_{cr}, T_{cr}) can be written in terms of the microscopic parameters a and b: $V_{cr}=3b$, $p_{cr}=a/(27b2)$, and $T_{cr}=8\mu a/(27Rb)$, where μ is the molecular mass and R is the universal gas constant. We define the dimensionless variables: $\Pi=p/p_{cr}$, $\Theta=T/T_{cr}$, and $Q=V/V_{cr}$. The Hugoniot curve is characterized by the initial state of the upstream gas (Π_1, Q_1) and its final state (Π_f, Q_f). After some algebra, we arrive at the equation for the Hugoniot curve:

$$\Pi_f \equiv \Pi_f(Q_f,Q_1) = \frac{\frac{\sigma_1}{8}\left[\left(\Pi_1+\frac{3}{Q_1^2}\right)(3Q_1-1)-3\frac{3Q_f-1}{Q_f^2}\right]}{\frac{\sigma_1}{8}(3Q_f-1)-\frac{3}{16}\left(\frac{Q_f}{Q_1}+1\right)Q_1+\frac{3}{8}Q_f} + \frac{\frac{9}{8}\left(\frac{1}{Q_f}-\right)+\frac{3}{8}-\frac{3}{16}\left(\frac{Q_f}{Q_1}+1\right)}{\frac{\sigma_1}{8}(3Q_f-1)-\frac{3}{16}\left(\frac{Q_f}{Q_1}+1\right)Q_1+\frac{3}{8}Q_f}. \tag{45}$$

The dimensionless DK parameter can be written in terms of the derivative of Π with respect to Q along the Hugoniot curve, in the final state:

$$h = \frac{6\beta_s^2}{Q_f^2}\left(1+\frac{1}{\sigma_1}\right)\left(\frac{3+\Pi_f Q_f^2}{6Q_f-2}-\frac{1}{Q_f}\right)\left(\frac{d\Pi_f}{dQ_f}\right)^{-1}. \tag{46}$$

An additional requirement is that when taking the gas from its initial to its final state, the curve that joins both states be inside the region defined by the condition $(\partial^2 V/\partial p^2)_s > 0$ [44]. Otherwise, the front will not be compressive [2,3,6,44].

B. Temporal evolution of the perturbations: Series of Bessel functions [Eq. (7)]

1. Pressure perturbations at the shock front

In this subsection, we use the results of Sec. II to get the evolution of the pressure perturbations as a function of time. The goal is to use the series of Bessel functions indicated in Eq. (7). To collect the information necessary to deal with a specific case, we must calculate the coefficients π_{2n+1} with the help of Eqs. (12)–(14). The initial state has a specific volume $Q_1=3$, which gives us a dimensionless pressure $\Pi_1=0.667$, having assumed that the temperature is equal to the critical temperature $(\Theta_1=1)$. In Fig. 3 we show the behavior of the pressure perturbations for this case as a function of the distance traveled by the shock from the piston. The final compression volume is $Q_f=1$. The upstream Mach number is $M_1 \approx 1.262$ and the downstream Mach number is $\beta_s=0.726$. It is clearly seen that after a short transient, the perturbations at the shock front oscillate with a definite amplitude and frequency. There is qualitative agreement with the observations of Bates and Montgomery [7]. With the series expansion used here, we can only measure the amplitude and frequency of the oscillations directly from the graphic itself. Nevertheless, in the next section we will do the same job by making an inverse Laplace transformation of the results obtained in Sec. III, calculate them analytically, and compare them with the results obtained in this subsection. For the

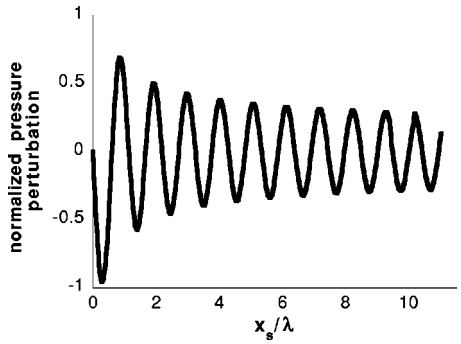

FIG. 3. Dimensionless pressure perturbations at the shock front as a function of the distance traveled by the shock in units of λ. The gas parameters are $\sigma_1=30$, $Q_1=3$, and $Q_f=1$.

same gas parameters, we show the DK function h_c-h in Fig. 4, as a function of the upstream Mach number. We see that this function is negative for some range of the final volume, which means that the DK mode can be excited there. Indeed, this is the case, as seen in Fig. 4. Regarding the other modes, it can be seen that the quantity $h_{c2}-h$ is never negative for this Hugoniot curve, and thus the second mode cannot be excited. However, as has been discussed previously, we could excite the additional modes at higher compressions. It is clear that it would be convenient to start with an initial state far from the liquefaction curve, in the ideal gas zone of the fluid, and choose a final state, near the phase transformation curve, without ever crossing the $G=0$ line. The next case we plot is a shock moving into a real gas with $\sigma_1=80$ and initial volume $Q_1=35$. The initial temperature is always equal to the critical temperature. In Fig. 5, we plot the corresponding parameters h_c-h, $h_{c1}-h$, and $h_{c2}-h$ to search for the zones in the space of physical parameters in which there is the possibility of exciting the DK mode, the second mode, the piston mode, or all of them. As can be seen, the range of final volumes, and hence of upstream shock Mach numbers, in which the second mode is excited is smaller as compared to the analogous interval for the DK mode. The shock Mach numbers necessary to excite the second eigenmode are, in fact, larger. According to these results, we should observe both modes of shock oscillation together, for example at a final compression volume $Q_f=1$. In Fig. 6 we plot the pressure perturbations at the shock front. The upstream Mach number is $M_1\approx 4.59$ and the downstream Mach number is

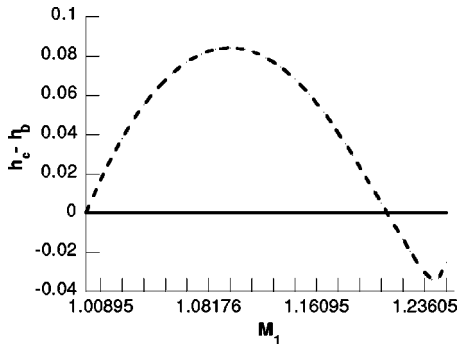

FIG. 4. Parameter h_c-h_D as a function of the upstream Mach number.

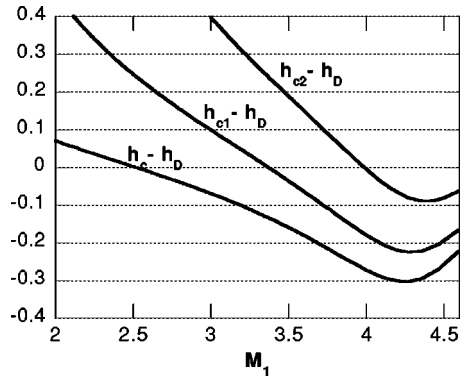

FIG. 5. Parameters h_c-h_D, $h_{c1}-h_D$, and $h_{c2}-h_D$ as functions of the upstream Mach number.

$\beta_s\approx 0.215$. We see that there is a modulation of the perturbations due to the action of, at least, two different eigenmodes. If we calculate the upper bound of Eq. (35) for this case, we get $n\leqslant 1.23$, which means that the factors $1/[\cosh(q+2j\theta_s)-\alpha_1(q+2j\theta_s)]$, with $j\geqslant 2$, do not have poles. Thus, only one additional mode, besides the DK mode, is possible for this Hugoniot.

2. Pressure perturbations at the piston surface

As for the piston perturbation concerns, we have only imposed that the normal velocity perturbations are zero. It does not mean that every other quantity is zero, even asymptotically in time. That this is so is clear from the results of Sec. III, in which we have seen that the Laplace transform of the pressure fluctuations could show a number of poles when evaluated at the piston. That is, there could be an asymptotic oscillatory behavior for those perturbations. They are the result of the interference of all the waves emitted by the shock downstream. For certain conditions, the piston becomes a surface where those waves could interfere constructively and the amplitude would neither grow nor decrease in time. To confirm these facts, we can see in Fig. 5 the parameter $h_{c1}-h$ as a function of the upstream Mach number. It is clear that we will find pressure oscillations at the piston, at higher compressions than are necessary for the standard DK mode at the shock front. Correspondingly, a lesser compression is required than that which is necessary to excite the second shock eigenmode. In Fig. 7 we show the temporal evolution,

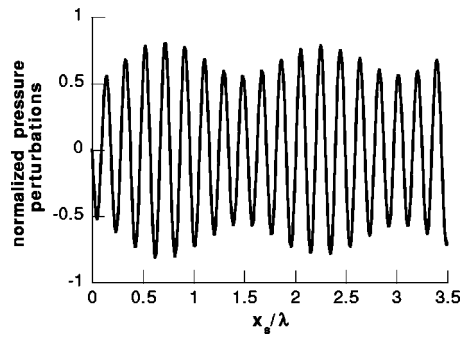

FIG. 6. Dimensionless pressure perturbation at the shock front. The gas parameters are $\sigma_1=80$, $Q_1=35$, and $Q_f=1$.

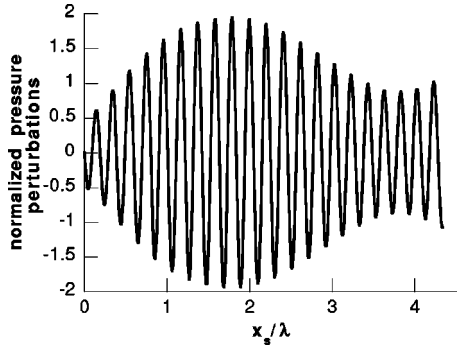

FIG. 7. Dimensionless pressure perturbation at the piston surface ($x=0$), for the same gas parameters as in Fig. 6.

calculated with the series expansion given by Eq. (7), for a shock moving into a real gas with a dimensionless specific heat $\sigma_1=80$, $Q_1=35$, and final volume $Q_f=1$. The modulation seen on the signal is due to the interference of the characteristic oscillation at the piston with the transverse sound waves that travel in the resting fluid with frequency kc_f [10].

C. Residues at the poles

1. Single DK mode at the shock front

We want to compare the previous results with the analytical information that can be derived from the Laplace transforms calculated in Secs. III and IV. As we know from the theory of the Laplace transform [40,46], the shock pressure perturbations in the real time domain can be calculated with the following integral in the complex plane:

$$\delta\hat{p}_s(r)=\frac{1}{2\pi i}\int_{z-i\infty}^{z+i\infty}\delta P_s(s)e^{sr}ds, \tag{47}$$

where z is a real number chosen in such a way that all the singularities of the integrand lie to the left of the line Res $=z$. As δP_s is a Laplace transform, it vanishes for large values of its argument. Then, if we close the path of integration with a large semicircle to the left, the integrand approaches zero at least as fast as $e^{(\mathrm{Res})r}$ with $\mathrm{Res}<0$ and the residue theorem can be used to calculate the integral in Eq. (47) [46]. That is, we choose a suitable contour Γ which closes the vertical path of Eq. (47) to the left, and formally write the equation [46]

$$\frac{1}{2\pi i}\oint_{\Gamma}\delta P_s(s)e^{sr}ds=\int(\text{residues at the poles})+\oint(\text{around essential singularities}). \tag{48}$$

Instead of dealing with the variable s it has proved more useful to work with the variable w, as suggested by Miller and Ahrens, which is defined by [5]

$$s=\frac{1}{2}\left(w-\frac{1}{w}\right). \tag{49}$$

The variable w is essentially the same as the variable y used by Fraley [10]. We must also choose a closed path that encircles all the singularities of the integrand in the w plane. We consider first the simplest situation studied in the previous subsection. Let us consider a corrugated shock moving into an undisturbed van der Waals gas with dimensionless heat capacity given by $\sigma_1=30$, initial volume $Q_1=3$, and final volume $Q_f=1$. We want to reproduce the results of Fig. 3 with the theoretical tools given by the preceding equations.

The contour integral can be rewritten in the w plane as

$$\frac{1}{2\pi i}\oint_{\Gamma}\delta P_s(s)e^{sr}ds=\frac{1}{2\pi i}\oint_{\Gamma'}\delta P_s(w)\left(\frac{w^2+1}{2w}\right)e^{(r/2)(w-1/w)}\frac{dw}{w}. \tag{50}$$

The circuit Γ' is the corresponding contour in the w plane. For the case studied in Fig. 3, the Laplace transform has two poles at $s=\pm is_0$, which correspond to two poles $\pm iw_0$ in the w plane. There is also an essential singularity at the origin in the w plane, due to the exponential term. The integration path reduces to two small circles of arbitrarily small radius that enclose the poles $\pm iw_0$, and a circle of radius unity that surrounds the origin clockwise, due to the essential singularity there. Thus, after some manipulation, the function $\delta\hat{p}_s(r)$ can be calculated:

$$\delta\hat{p}_s(r)=\delta\hat{p}_{s0}(r)+\frac{1}{2\pi i}\oint_{C}\delta P_s(w)\left(\frac{w^2+1}{2w}\right)e^{(r/2)(w-1/w)}\frac{dw}{w}, \tag{51}$$

where $\mathcal{C}$ is a circular path enclosing the origin clockwise, and $\delta\hat{p}_0(r)$ is the contribution due to the simple poles $\pm iw_0$. To calculate $\delta\hat{p}_{s0}$ we must manage the terms that contain the factor $\cosh q-\alpha_1(q)$. It is useful to factorize it in terms of the variable w in the form

$$\cosh q-\alpha_1(q)\equiv\frac{(1-\alpha_{10})}{2w(w^2-1)}(w-iw_0)(w+iw_0)\times(w-i\zeta_0)(w+i\zeta_0), \tag{52}$$

where $\zeta_0=\sqrt{U_0}e^{-2\theta_s}$, with $U_0=[-\sqrt{1+4\alpha_{11}(\alpha_{11}-\alpha_{10})}+\alpha_{10}-2\alpha_{11}]/(1-\alpha_{10})$. We write the final result for the pole contribution, after some long algebra, as

$$\delta\hat{p}_{s0}(r)=a_0\sin s_0r, \tag{53}$$

which gives a sinusoidal contribution as expected, since $\delta\hat{p}_s(r=0^+)=0$. The quantity a_0 is given in the Appendix. The next step is to calculate the integral along the unit circle. By simple inspection in the expression of δP_s in Eq. (19), it is clear that retaining a large number of terms in the calculation would be a difficult and not necessary task. This is due to the fact that the Mach number in this case is near unity, and with just the first term λ_1 is accurate enough. Actually, as θ_s is larger than unity, we could even approximate λ_1 by the term $\alpha_2(q)/[\cosh q-\alpha_1(q)]$ with negligible error in the final re-

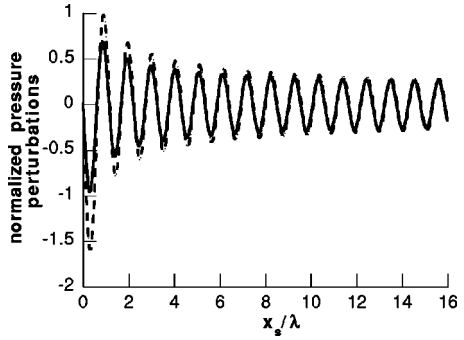

FIG. 8. Comparison of the exact (dash-dotted curve) and the asymptotic solution (solid curve) for the oscillations shown at the shock surface in Fig. 3.

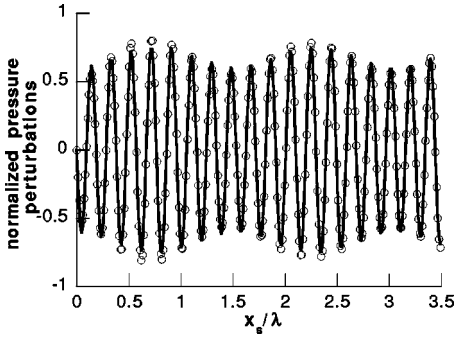

FIG. 9. Comparison of the exact (small empty circles) and the asymptotic solution (solid curve) for the oscillations shown at the shock surface in Fig. 7.

sults. This is what we do next, and later on compare with the exact result given by the series of Bessel functions. Making the substitution $w=e^{i\phi}$ and after using symmetry properties of the trigonometric functions involved, the integral around the contour C is reduced to

$$\frac{1}{2\pi i}\oint_C \delta P_s(w)\left(\frac{w^2+1}{2w}\right)e^{(r/2)(w-1/w)}\frac{dw}{w}$$

$$=\frac{1}{2\pi(1-\alpha_{10})}\int_{-\pi}^{\pi}\frac{2\cos\phi(1-w_0^2\zeta_0^2)(\sin 2\phi+w_0^2+\zeta_0^2)}{(1+2w_0^2\,2\phi+w_0^4)(1+2\zeta_0^2\cos 2\phi+\zeta_0^4)}$$

$$\times\sin(r\sin\phi)d\phi. \tag{54}$$

In Fig. 8, we compare the solution given by the series of Bessel functions used in the last subsection and the results predicted by Eqs. (53) and (54). We see that the agreement is very good, except during the transient stage when the shock is still near the piston surface. As the effect of the sound wave reverberation is important when the shock is still near the piston, we would need at least the complete expression for λ_1 to take into account these early time reflections. Anyway, due to the small value (near unity) of the Mach number, the difference from the exact solution is quite small, after the shock separates from the wall some wavelengths. The numerical values of the complex poles predicted by our equations are $w_0\approx 1.073$ and $s_0\approx 1.0025$. To calculate the temporal frequency associated with the poles $\pm is_0$ we must go from the r variable back to the t variable. This amounts to dividing by $\cosh\theta_s\approx 1.454$. We thus obtain the temporal frequency of the oscillations in units of kc_f: $\omega_0=s_0/\cosh\theta_s\approx 0.689kc_f$. We multiply it by the factor $2\pi/\beta_s$ to get the spatial frequency $2\pi\omega_0/\beta_s\approx 5.965$. This gives us a spatial period (the horizontal axis is the shock-piston distance divided by the perturbation wavelength) equal to $\beta_s/\omega_0\approx 1.053$, which coincides very well with the result shown there.

2. First and second modes at the shock front

We increase now the Mach number and the specific heat to compare with the results presented in Fig. 8. We consider a real gas with $\sigma_1=80$, $Q_1=30$, and $Q_f=1$. We have now a second pair of complex conjugated imaginary poles $\pm is_2$, as given by Eq. (33). These poles in the s plane correspond to an equivalent set of two complex conjugate poles $\pm iw_2$ in the w plane. We have $w_2=\sqrt{T_2}=\sqrt{T_0}e^{-2\theta_s}$, with T_2 given by Eq. (34). Analogously to the situation found for the first DK eigenmode, the absolute value of the previous pole is larger than unity. In addition, there are two additional zeros of the factor $\cosh(q+2\theta_s)-\alpha_1(q+2\theta_s)$, which have absolute values less than unity and which we call $\pm i\zeta_2$. They correspond to a negative α value, which is related to the negative determination of the square root in terms like $\sqrt{s^2+1}$, and are therefore excluded as poles of our Laplace function. The main difference from the last section is that we have now two additional terms in the residue calculation. The residues associated with the poles $\pm is_0$ are calculated in the same way as before. To deal with the second poles, it is more convenient to define a new auxiliary function that factors out the denominator $1/[\cosh(q+2\theta_s)-\alpha_1(q+2\theta_s)]$. After some considerable algebra, we get

$$\delta\hat{p}_{s2}(r)=a_2\sin s_2 r, \tag{55}$$

where the quantity a_2 is given in the Appendix. The total shock front pressure perturbation will be given by a sum of the form

$$\delta\hat{p}_s(r)\equiv\delta\hat{p}_{s0}(r)+\delta\hat{p}_{s2}(r)+\frac{1}{2\pi i}\oint_C\delta P_s(w)$$

$$\times\left(\frac{w^2+1}{2w}\right)e^{(r/2)(w-1/w)}\frac{dw}{w}, \tag{56}$$

where the integral in the right hand side is the contribution of the essential singularity at the origin and gives rise to decaying oscillations superposed on the permanent, stable oscillations given by the simple poles $\pm is_0$ and $\pm is_2$.

We show the final result in Fig. 9. It is noted that only the asymptotic contribution given by the oscillatory terms has been included. We see that it introduces only a small difference during the transient stage, when shock and piston are quite close ($x_s\sim\lambda$). The numerical values for this case are $w_0=1.714$, $s_0=1.149$, $w_2=1.108$, and $s_2=1.005$. We clearly see the modulation due to the simultaneous excitation of both frequencies. A natural question is to ask whether it is possible to have an excitation in which the amplitude of the standard DK mode could be smaller compared to the ampli-

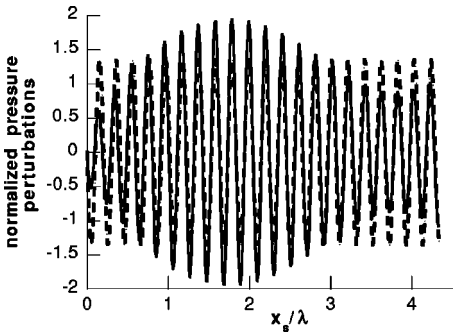

FIG. 10. Comparison of the exact (dashed curve) and the asymptotic solution (solid curve) for the oscillations shown at the piston surface in Fig. 9.

tude of the second mode. At least for the zone of the space of parameters explored here, it does not seem feasible.

D. Pressure oscillations at the piston

As has been shown in Eqs. (36) and (37), the piston pressure Laplace transform also satisfies a functional equation, from which an exact particular solution can be found. The imaginary poles of that solution would correspond to stable oscillation modes at the piston surface. It is not difficult to understand that the poles are given by the zeros of terms of the form $\cosh[q+(2n+1)\theta_s]-\alpha_1[q+(2n+1)\theta_s]$. To show a specific case, we study the same real gas as in the previous section (Fig. 9) and the final volume is now $Q_f=1$, such that the first eigenmode at the piston is excited. The poles are at $\pm is_1$, with $s_1=1/2(w_1+1/w_1)$ where $w_1=\sqrt{T_0}e^{-\theta_s}$. The calculations of the residue at the previous pole are entirely similar to the algebraic steps done for the first DK eigenmode at the shock. The function $\delta\hat{p}_{i0}(\tau)$ is given by

$$\delta\hat{p}_{i0}(\tau) = a_1 \sin s_1\tau, \tag{57}$$

where the quantity a_1 is also given in the Appendix. In Fig. 10 we show the results given by the series of Bessel functions and compare them with the function $\delta\hat{p}_{i0}(\tau)$ for the same situation studied in Fig. 7. We see that the perturbation is modulated by another signal that oscillates at the frequency kc_f. This is the natural frequency of the transverse sound waves that exist near the piston and travel almost parallel to it, as discussed by Fraley [10]. This modulation will later decrease in amplitude, and the asymptotic perturbation will be the stable oscillation given by the contribution $\delta\hat{p}_{i0}$ above. As the shock is rather strong in this case, the effect of the transverse sound waves is not negligible. This contribution comes from the integral along the unit circle in the complex w plane and takes longer to attenuate. For this case, we have $w_1=1.378$ and $s_1=1.052$. The spatial period (when measuring the perturbations as a function of x_s/λ) is $\beta_s/s_0 \approx 0.214$. On the other hand, the period of oscillation of the modulating envelope would be approximately given by $\beta_s/(s_1-1)\approx 4.146$ which coincides quite well with the value directly measured in Fig. 12 below. Thus, it would take at least two or perhaps more of such time intervals in order for the modulation produced by the transverse waves to decay considerably and leave space to the dominant piston eigenmode. It is interesting to make here a brief digression about the mathematical origin of the modulation seen in Fig. 7 or 10. Its nature is quite different from the modulation seen on the shock perturbations in Fig. 6 or 9. In the case of the shock perturbations, we have the excitation of two simultaneous eigenfrequencies which correspond to the terms $\delta p_0 \propto \sin s_0 r$ and $\delta p_2 \propto \sin s_2 r$ in Eq. (56). In the piston case, studied in Figs. 9 and 12, we have only one eigenfrequency, given by the conjugated poles $\pm iw_1$, or equivalently $\pm is_1$. If we look more closely at the expression of $\chi_1(q)$, we would see that there is a term $\cosh q \equiv \sqrt{s^2+1}$ in the denominator, which is not present in the expression for $\delta P_s(q)$, in Eq. (19). We could always formally calculate the inverse Laplace transform of the new function $\delta Y(q)=\cosh q\,\delta P_i(q)$ from Eq. (36). It is clear that this new function δY would give rise to the same poles as δP_i but different residues. In fact, after some tedious algebra, it can be seen that the inverse Laplace transform of δY is proportional to a function of the form $\cos s_1\tau$, which is different from the sine behavior associated with the poles of δP_s and δP_i. But we are interested in the inverse of $\delta Y(q)/\cosh q \equiv \delta Y(s)/\sqrt{s^2+1}$. It is then immediate that part of the asymptotic response of $\delta\hat{p}_i$ would be given by a convolution of $\cos s_1\tau$ with $J_0(\tau)$, where J_0 is the ordinary Bessel function of zero order [40,46]. This explains the modulation at the piston.

V. DISCUSSION

A. Comparison with previous works

It will be interesting to review former works that have also used the Laplace transform technique. We want to understand where the previous works separate from our conclusions and where they agree. The Laplace transform approach has been used initially by Roberts [20] to study the propagation of an isolated shock into an ideal gas. Recently, the same approach has been followed and mistakes in the original work of Roberts have been corrected [47]. In it, the author tries to study the instability problem for a shock moving into a fluid with arbitrary equation of state. The idea used is the same as the one used here, to look for the poles of the Laplace transform and search for the conditions under which unstable behavior could be observed. Zaidel' also used the Laplace transform to solve the perturbation problem ahead of a corrugated piston, and has been the first to propose, to our knowledge, the Lorentz transformation that leads to Eq. (6). Later on, the same approach was used to study the reflection of a planar shock from a corrugated wall and compare the theoretical predictions with experimental results [35]. Much later, in the context of the Richtmyer-Meshkov instability, Fraley (after Zaidel') has provided the scientific community with a rigorous, complete, and exact analytical solution for the perturbation field evolving between two shocks separated by a corrugated contact surface, in ideal gases. His approach, however, dealing with the same physics as here, managed the fluid equations in the physical space of the x, t variables, making a Laplace transformation in time, instead of working with Zaidel's coordinates r, θ. We will later see that his ap-

proach and ours are entirely equivalent, and therefore, our conclusions could also be obtained following his calculations. Unfortunately, he restricted his analysis only to ideal gases, and did not show any quantitative result regarding a stability criterion like Eq. (2) or Eq. (30). Some years later, Miller and Ahrens [5] applied and improved Zaidel's work with a more or less similar formalism as the one used in this work, to address the effect of viscosity on the shock perturbation evolution. It is also interesting to briefly review this work, as the authors have considered a perturbed shock moving into an inviscid fluid too. Nevertheless, they used an approximate boundary condition at the piston surface, namely, that the eigenmodes should vanish there, on the assumption that for large times, shock and piston would be separated far enough and any causal influence between them could be safely neglected. It is interesting to notice that in so doing, they do not get a functional equation for their Laplace transform and therefore they can only predict the standard DK mode. On the contrary, the work done by Fraley does include consistent boundary conditions at both the piston and the shock front and obtains a functional equation completely equivalent to our Eq. (15). We start by discussing very briefly the derivations of Miller and Ahrens for their inviscid case. After that, we continue with Fraley's work.

1. Isolated shock (Miller and Ahrens' work, Ref. [5])

According to Ref. [5], we could take the Laplace transform of the fluid equations and write them in the following compact form:

$$\frac{\partial \vec{u}}{\partial x} = A\vec{u}, \tag{58}$$

where u is a three-component vector defined essentially by $\vec{u}=(\delta u, \delta v, \delta P)$, with δu the Laplace transform of the perturbed normal velocity, δv that of the tangential direction, and δP that of the pressure perturbations. Their dimensionless quantities are defined with different scaling factors, so our comparison remains qualitative. In addition, they use a coordinate frame moving with the shock. The tensor A is 3×3 matrix whose components can be found in Ref. [5]. Our aim is only to make a simple discussion that points out the differences in their results as compared with ours, and try to understand the reasons for that difference. They propose a general solution of the form $\vec{u}=\vec{u}_{x=0}e^{\lambda x}$, where it is remembered that $x=0$ is the shock position in their frame of reference. The quantity λ is a possible eigenvalue for the differential equations system of Eq. (58). After inserting the previous ansatz in the equations, the three eigenvalues $(\lambda_1,\lambda_2,\lambda_3)$, and their associated eigenvectors can be obtained. The matrix A can then be factorized as

$$A = S^{-1}\Lambda S, \tag{59}$$

where S is a matrix formed by the eigenvectors and Λ is the diagonal matrix formed with the eigenvalues. The original Eq. (58) can then be recast as

$$\frac{\partial \vec{u}}{\partial x} = S^{-1}\Lambda S\vec{u}. \tag{60}$$

The last equation can be formally solved, to obtain

$$\vec{u} = S^{-1}e^{\Lambda}[(S\vec{u})_{x=0}]. \tag{61}$$

The previous equation gives us the three perturbation quantities in terms of the three eigenvalues of the problem and the boundary conditions at the shock. However, since their third eigenvalue is positive, the exponential $e^{\lambda_3 x}$ will diverge in the limit $x\to\infty$. To circumvent this apparent difficulty, the authors assume that the corresponding eigenvector should vanish, in order to keep a bounded solution in the whole space behind the shock ($x>0$ means behind the shock in their notation). This approximate boundary condition is somewhat equivalent to "forgeting" the piston in the compressed fluid and not considering any reflecting surface at all. After adopting this approximation, they managed to obtain a mathematical solution for the shock front ripple. In analyzing the poles of that solution, they obtain the DK criterion for the emission of undamped sound waves [their Eq. (27)]. That is, when forcing the piston behind the shock to completely decouple from the shock, we are erasing from the problem the sound wave reverberations that take place between the shock and the piston after $t=0^+$. In other words, we are excluding from the problem, from the very beginning, the ingredient that excites the rest of the spectrum. Only the DK mode will be retained, because it actually does not need any sound wave coming from behind.

2. Shock interacting with a contact surface (Fraley's work, Ref. [10])

In connection with the work of Miller and Ahrens, we discuss now the work of Fraley, which makes essentially the same mathematical treatment: he takes the temporal Laplace transform of the equations of motion and integrates them in space. He obtains the sound pressure modes (essentially, the modes associated with the same eigenvalues λ_2 and λ_3 of Miller and Ahrens) and stationary vortex and entropy modes [10]. The main difference between these two works, besides notation, is that Fraley did not exclude the piston from the mathematical formulation. He used the correct boundary condition regarding the normal velocity component there and the continuity of pressure (in case there were another fluid to the left of the piston surface, as in the standard Richtmyer-Meshkov problem). In so doing, he had to keep account of the Doppler shift at the shock fronts, because at some point in the calculations we must couple the shock oscillations with the fluctuations that arise in the resting fluid near the piston. This mathematical complication (apparent in the value of the eigenvalues λ_2 and λ_3 of Ref. [5]) would be always present, and it is responsible for complicating the mathematical structure of the equations in such a way that the Laplace transform would be the solution of a functional equation. If the physics included in Fraley's work is the same as ours, then we should also reobtain our Eq. (15) with Fraley's equations. This is our next task in the following lines. To keep the notation as simple as possible, we try to follow Fraley's nomenclature, except when it is no longer possible

to do so. Let us begin with the mathematical structure of the modes found in Ref. [10]. The pressure modes are written as [10]

$$\delta p(s,x) = a(s)\exp(x\sqrt{s^2+1}) + b(s)\exp(-x\sqrt{s^2+1}), \tag{62}$$

from which the corresponding perturbations in normal (δu) and tangential (δv) velocities can be derived. There is a third mode that accounts for the generation of vorticity and another for the generation of entropy at the corrugated shock. As discussed by Fraley, the first mode $[a(s)\exp(x\sqrt{s^2+1})]$ consists of waves escaping from the shock into the compressed fluid. The other mode $[b(s)\exp(-x\sqrt{s^2+1})]$ stands for the sound waves that hit the shock from behind. Furthermore, to deal with the moving shock front, the transform of the pressure at the shock must be rewritten by using a common Laplace variable which Fraley calls r, but which we prefer to call $\hat{r}$ in order not to confuse it with our Lorentz coordinate in Eq. (6). To understand the origin of the common variable $\hat{r}$, it is better to write the inverse Laplace transform of one of the modes at the shock [10]:

$$\int_{z-i\infty}^{z+i\infty} ds_2 a(s_2)\exp(s_2\tau + \beta_s\tau\sqrt{s^2+1}) = \int_{z-i\infty}^{z+i\infty} d\hat{r}\, a(s_2)\frac{ds_2}{d\hat{r}}\exp(\hat{r}\tau), \tag{63}$$

and analogously with the other mode $b(s_1)$. We see that the frequencies of oscillation of the modes $a(s)$ and $b(s)$ at the shock front are Doppler shifted. We also recognize the factor $\sqrt{s^2+1}$, which enters naturally into the problem. Its origin resides in the transverse partial derivative $\partial^2 p/\partial y^2$ in the wave equation [Eq. (6)]. That is, the term $\sqrt{s^2+1}$ and the branch points associated with it (at $s=\pm i$) are the mathematical manifestation of the existence of a lateral flow along the transverse direction y.

The Laplace variables s_2, s_1, and $\hat{r}$ are connected by

$$\hat{r} = s_2 + \beta_s\sqrt{s_2^2+1},$$

$$\hat{r} = s_1 - \beta_s\sqrt{s_1^2+1}. \tag{64}$$

Let us define $s=\sinh q$, $s_2=\sinh q_2$, and $s_1=\sinh q_1$. It is easy to obtain, after some algebra,

$$\hat{r} = \frac{\sinh(q_1-\theta_s)}{\cosh\theta_s} = \frac{\sinh(q_2+\theta_s)}{\cosh\theta_s}. \tag{65}$$

That is, $q_1=q_2+2\theta_s$. Therefore, the Laplace transform of the pressure perturbations at the shock, according to his notation, is

$$\delta P_s(\hat{r}) \equiv a(q-\theta_s)\cosh(q-\theta_s)\frac{\cosh\theta_s}{\cosh q} + b(q+\theta_s) \times\cosh(q+\theta_s)\frac{\cosh\theta_s}{\cosh q} \equiv \frac{f_1(q-\theta_s)+f_2(q+\theta_s)}{\cosh q}. \tag{66}$$

which coincides with our solution, later shown in Eq. (70). To show the complete equivalence between Fraley's calculations and ours, we have to go to the boundary conditions at the shock front [37] [namely, his Eqs. (14) and (15)] and reobtain our Eq. (15). When manipulating his shock boundary conditions, in the same way as Richtmyer did, to get a differential boundary condition for the pressure fluctuations, we arrive at

$$[\hat{r}^2 - (\beta_s+E_1)\cosh(q-\theta_s)\hat{r} - E_2A_\psi]f(q-\theta_s) + [\hat{r}^2 - (\beta_s+E_1)\cosh(q+\theta_s)\hat{r} - E_2A_\psi]f(q+\theta_s) = E_2\psi_0\frac{\cosh\theta_q}{\cosh\theta_s}. \tag{67}$$

To get the last equation, we have made use of the only acceptable boundary condition at the rigid piston, namely, $f_2=f_1=f$, because the normal acceleration is zero at the wall. After some additional lengthy algebra, which we prefer not to show, it is straightforward to see that the previous equation is the same functional equation as Eq. (15), when rewritten in terms of our function $F=F_1=F_2$. Some immediate conclusions can be drawn from this result. It is clear that with either Fraley's approach or the model presented here, we would get the same spectrum for the perturbed shock and the fluctuations that evolve in the downstream fluid. That is, we would reobtain the same oscillation patterns at the shock and at the piston. He continued his analysis further and discussed the question of stability of the shock traveling in ideal gases in the context of the Richtmyer-Meshkov instability and obtained well known results [47,48]: temporal decay like $\tau^{-3/2}$, etc. We will not review those issues here. We want to emphasize the fact that, when considering a reflecting surface behind the shock, a term that describes the reflected waves must be included and a functional equation for the Laplace transform of the pressure appears naturally. As can be deduced from Eqs. (62)–(67) the nature of the functional equation is the Doppler shift at the shock front and the existence of a reflecting surface behind it. Furthermore, if we want to close the problem and solve it exactly, we need an additional condition on either f_1, or f_2, or both functions. That is, we should say something about either the left facing, the right facing, or both types of waves. In the case of a rigid piston, we ask for the vanishing of the normal acceleration there. On the contrary, if the piston were a free surface, a situation in which the pressure perturbations would be zero there all the time (but not the normal velocity perturbations; this is the symmetrical Riemann problem discussed by Velikovich [41]), we would require: $f_1=-f_2=f$ [9,36,37,41]. On the other hand, if the shock were traveling isolated, without interacting with a wall from behind, a case also discussed by

Fraley [10] and used as a paradigm by many others [1,5–7,20–24,26–33,47,48], we should make the second Fraley mode $b(s_2)=0$, which is consistent with making $F_2 \equiv 0$ in our notation. This boundary condition behind the shock erases completely the right facing waves that hit the shock from behind. As will be clear from the discussion in the next section, with this assumption, no additional modes other than the DK mode would be excited. Going back to the Miller and Ahrens work, it is clear that they would also have been able to get the complete spectrum if they had retained the reflecting surface behind the shock, in much the same way as Fraley did to deal with the shock and piston boundary conditions. As they were interested in other phenomena inside the viscous fluid into which the shock was propagating, they considered a good starting point to neglect the piston boundary, in order to simplify the discussion at the shock.

Before concluding this paragraph, we reconsider the normal mode approach used to derive the classical DK criterion. As we know, to solve a partial differential equation by separation of variables, some conditions must hold not only for the equation itself but also for the boundaries. The wave equation is known to be separable, and this justifies at least the ansatz done in Eq. (4). But the boundaries should be *rectangular* in the system of coordinates chosen [49–51]. That is, the boundary conditions should be known at fixed values of the coordinates, in order to define Sturm-Liouville problems in at least one of them, and get orthonormal sets of functions. After a linear superposition, the solution to the problem can be found by application of the boundary and initial conditions [49–51]. But, for the method to work properly, the boundaries in the x or y directions should be kept constant in time (either a constant real number, or just taken at infinity). In the case of the shock problem discussed here, in the reference frame used, the shock surface is moving: $x_s(t)=u_s t$. This fact precludes the use of separation of variables to solve the problem in Cartesian coordinates, if we want to consider the piston and the shock together. To avoid this complication, we have used a Lorentz transformation [see, for example, Eq. (6)]. In the new system of coordinates, the domain of integration is the union of "squarelike" intervals of the form $0 \leqslant r < \infty$ and $0 \leqslant \theta \leqslant \theta_s$. In this way, we arrived at well known equations: the Bessel equation for the r variable, with a complete system of solutions, and the spring equation in the variable θ, for which exponential solutions can be derived. After superposing both sets of functions, we calculated the coefficients of the expansion by applying the boundary and initial conditions both at the piston and at the shock. The solution is presented in the form of a series like Eq. (7). It is clear that nonlocality in space and time is a characteristic of the solution that is unfortunately necessary to explain the subtleties of the perturbation field between both surfaces [see, for example, the works of Roberts [20] or Bates [47] to see the causal influence between shock and piston, propagated along characteristic rays in the x,t space]. The solution indicated in Eq. (7) has all the physics, once the coefficients D_ν are calculated. What happens then, with a perturbation of the form suggested by Eq. (4)? We know that by assuming this type of solution in the Rankine-Hugoniot conditions, the stability condition for spontaneous acoustic emission [Eq. (2)] is correctly obtained [1,6,7]. However, the more general criterion for the possible excitation of the complete (finite) spectrum is lost. We could reconcile these two results thanks to the conclusions of the model developed here. In fact, let us consider, for example the derivation of the dispersion relation as done in Ref. [26]. In it, the origin of coordinates is taken at the shock itself. Then, the piston moves to the left with a finite velocity and spoils the use of the separation of variables. However, we could formally suggest a separated solution like Eq. (4) if the piston boundary were at infinity. In fact, "Since it takes a finite time for the perturbation to interact with the medium at a large distance from the shock, we impose the physical constraint on the perturbation quantities that they die out at sufficiently large distances. Mathematically, this is equivalent to a requirement on the *separation of variables solution* that it be bounded as $x' \to \infty$", as extracted from Ref. [26]. Assuming the piston very far away is equivalent to excluding from the problem the physics that occurs between shock and piston from $t=0^+$ onward, with the illusion that we would pick out the essential properties of the asymptotic behavior, just because we are studying the system in the limit $t \to \infty$. This would be the correct form of dealing with the asymptotic evolution if the system were capable of "forgetting" somehow the initial conditions quite soon, that is, if the problem were self-similar [2], which is certainly not the case here. It is also not true in more complex situations like the Richtmyer-Meshkov problem, in which the early time interaction between shock and contact surface decides the value of the instability rate of growth at later times [9,10,37]. As has been shown in previous sections, the acoustic emission modes exist together with the decaying perturbations from $t=0^+$. Therefore, letting the piston surface go very far to the left and making the perturbations there equal to zero is the same as erasing the right facing waves reflected by the piston and considering an isolated shock moving to the right. In this approximation, the solution will display only the standard DK mode, but not the rest of the possible frequencies. We note that setting $x'_{piston} \to \infty$ is the only way to justify the use of a separable solution. In conclusion, the usual approach developed by previous authors when studying the shock stability problem only gives a correct answer for an isolated shock front which does not interact with a reflecting boundary behind it. The more general problem of a shock with a reflecting piston surface shows a wider spectrum, which depends on the EOS of the fluid.

We should note that we could also find zones in which the shock exhibited another type of growth, maybe exponential. However, if we use the solution provided by Eq. (19), we must note that only the zones with $h < 1-2\beta_s^2$ are allowed to be explored. Therefore, we could study zones in which $h < -1$, in order to search for exponentially growing perturbations [1,26]. Of course, the zones with $h > 1+2\beta_s$ could also be explored with the same tools as here, but we need to include the solution to the homogeneous equation of Eq. (15), which has not been obtained yet for the 2D problem. Furthermore, as our analysis includes the piston, it is quite possible that an even wider spectrum than that predicted by Eqs. (68) and (69) could be found. This task is left for future work.

B. Classical DK dispersion relation

The approach followed in former works, since that of D'yakov and Kontorovich, has been the use of a (normal mode) separable solution for the perturbed quantities in the space behind the shock [1,5–7,21–33]. In doing so, the possibility of additional longitudinal wave numbers (along the $\hat{x}$ direction) must be taken into account. As we have seen in the last sections, the exact solution to the perturbed quantities cannot be written with separated x and t variables. The main reason is that we have to deal with the two types of sound waves: right and left facing. Even though we know that the DK mode is correctly predicted even when the approximate ansatz provided by a solution of the form $\exp(ik_x+ik_y y+\omega t)$ is used for the perturbation quantities. Another known approach to the shock stability problem has been to study the reflection of sound waves impinging on the shock front from behind [1,21–23]. In this way, the coefficient of reflection of the sound waves at the shock surface can be calculated from the linearized Rankine-Hugoniot equations. The conditions for spontaneous acoustic emission are obtained by requiring that the reflection coefficient becomes infinite. This requirement expresses the fact that the shock reflects sound waves in the absence of waves incident on it [22,23]. This has been another approach to obtaining Eq. (2). We have also obtained it here with a different formalism, by looking at the poles of the complete Laplace transform. The interesting task is understanding how to reconcile these approaches. Let ω be the oscillation frequency of the excited mode in the shock moving frame of reference. The fluid velocity that escapes downstream from the shock is u in the shock front system. Therefore, the frequencies measured at the shock and at the piston will not be the same due to the Doppler shift [1]. Let ω_0 be the frequency of the oscillations as measured in a system fixed to the piston surface. Then both frequencies are connected by [1,26]

$$\left(\frac{\omega_0}{k_y c_f}\right)^2 = \left(\frac{\omega}{k_y c_f} - \frac{k_x}{k_y}\beta_s\right)^2 = 1 + \frac{k_x^2}{k_y^2}. \tag{68}$$

In addition, we define $\hat{k}=k_x/k_y$ and $\Omega=\omega/(k_y c_f)$. The usual procedure is to introduce Eq. (4) into the linearized Rankine-Hugoniot conditions and obtain the dispersion relationship in the form [7,26]

$$D(\hat{k},\Omega) = 2\Omega\frac{\rho_1}{\rho_f}\left(1+\frac{\Omega^2}{\beta_s^2}\right) - \left(1+\frac{\rho_1}{\rho_f}\frac{\Omega^2}{\beta_s^2}\right)(\Omega-\beta_s\hat{k})(1+h) = 0, \tag{69}$$

and solve the last two equations together. It can be easily verified numerically that the first pole found in this work [Eq. (25)], which corresponds to the first acoustic emission mode, is a solution to the above dispersion relationship. However, the additional poles do not satisfy it. The reason is very simple and has to do with the kinematics of the interaction between the shock and the piston. As will be shown later on, the sound wave emitted at the DK frequency, is reflected at the piston surface with such an angle that it cannot get back to the shock. That is, the projection of its velocity along the normal to the shock is less than the shock speed. This result will be rigorously deduced in the next section when discussing the full spectrum. In consequence, as far as the dynamics of the standard DK mode is concerned, it is as if the piston did not exist. Once emitted by the shock, that mode will never interact with the shock after reflection at the piston boundary. Hence, it is easy to understand why the standard DK dispersion relation for the modes of an isolated shock agrees with our first pole at the shock found in this work. As will be shown later on, when the second mode is excited at the shock surface, the first mode is emitted at such an angle that it will definitely hit the shock from behind. In this way, the second mode appears because the first (standard DK mode) starts to interact with the shock, after reflection at the piston.

Let us briefly see how can we get the isolated shock acoustic mode within the framework of our model. The shock front pressure perturbations can always be rewritten as [34,37]

$$\delta P_s(q) = \frac{F_1(q-\theta_s)+F_2(q+\theta_s)}{\cosh q}, \tag{70}$$

where, as can be seen from Ref. [10] and the review presented in the last subsection, the function $F_1(q-\theta_s)$ stands for the sound waves that leave the shock surface into the compressed fluid. The second term $F_2(q+\theta_s)$ represents the waves that hit the shock from behind [10]. Therefore, in the absence of a true piston that can reflect sound waves, as in the example discussed by Bates and Montgomery [7], we must require that $F_2=0$ in the downstream fluid. From the boundary conditions at the shock and using the results of Ref. [37], $\theta=\theta_s$, we get a simple analytical solution

$$\delta P_s(q) = \frac{\alpha_2(q)}{\cosh q - \alpha_1}. \tag{71}$$

It is clear that with this boundary condition (no piston behind the shock), the solution is simpler than the one shown in Eq. (19). We also see that the Laplace transform given by Eq. (71) shows only one pole, if the conditions given by Eq. (2) are satisfied. That is, for an isolated shock, which is slightly perturbed in shape because of some infinitesimal shock tube width constriction, as in Bates and Montgomery [7], only the DK mode would be excited. Because there is no piston to reflect the sound waves in the space behind, the function $F_2=0$, and we lose the rest of the spectrum. That is, the sound waves that reverberate between shock and piston are necessary to excite the additional eigenmodes. Because the shock shape is corrugated, the shock will always start to oscillate at its highest natural eigenfrequency, as given by the DK prediction, when Eq. (2) is satisfied. However, in order to excite the other frequencies, we need the term $F_2(q-\theta_s)$. Otherwise, we would not be able to construct the functional equation [Eq. (15)], or its solution given by Eq. (19), and get the other eigenmodes. In other words, $F_2(q-\theta_s)$ is the term that keeps account of the waves that face toward the shock and it is a necessary ingredient to put the right facing sound waves in our system. This means that those waves should have been generated somewhere behind, at the piston surface. It is in this sense that we say that the left reflecting

boundary is necessary to excite the entire spectrum. In addition, the eigenmodes [represented by functions like $\delta\hat{p}_0(r)$ for the DK mode, or $\delta\hat{p}_2(r)$ for the second excited mode] exist from $t=0^+$. They are generated together with the rest of the perturbations once the corrugated shock has been formed, so it could be misleading to think of them as only an asymptotic response of the shock front. After the shock has traveled some wavelengths away, they will be the only remaining perturbations, because the contribution from the transverse and normal incidence sound waves [represented by the unit circle integral in Eq. (54), for example] would decay. Therefore, the spectrum, if the necessary conditions for its existence is satisfied, is fully excited from $t=0^+$. The first eigenmode exists without the need of having any sound wave coming from behind, because we got it even if $F_2=0$. On the contrary, the second eigenmode exists because $F_2 \neq 0$, thanks to the reflecting surface downstream [5,25,32]. We recall here that the possibility of including a reflecting surface behind the shock has been taken into account for the 1D problem, by Fowles and Swan in Ref. [25]. In it, the authors considered 1D perturbations in pressure that traveled along the characteristics, were reflected at the shock, and traveled back to the piston, to continue the reverberation process. It was shown, that depending on the EOS of the fluid, the shock front perturbations could either decrease, remain stable, or grow in time [25]. To sum up, we see that the excitation of these additional frequencies is a consequence of the reverberation of the sound waves that bounce between the shock and piston. This process starts very early in time, when shock and piston are very near each other (at $t=0^+$) and lots of reflections between piston and shock are taking place [12,41]. As discussed by Richtmyer [12], the effect of all those early time reverberations (at $t=0^+$) is to equalize the pressure between shock and piston, and make the total pressure perturbation nearly equal to zero initially. However, those initial reflections are also responsible for "exciting" the internal modes of the shock front in such a way that, if some of the inequalities in Eqs. (30) are satisfied, the shock starts to oscillate simultaneously with the corresponding spectrum, as has been shown in Fig. 9. In the next section we will show how these modes couple the shock and piston surfaces.

C. Shock-piston coupling

To start the discussion, let us follow a sound ray, reflected at the piston at some instant of time $\tau=\tau_0$. It has a wave vector (k_x,k_y) where k_y is the original perturbation wave number at the piston, and k_x is the longitudinal wave number associated with that mode. This vector forms an angle ϕ with the axis normal to the piston. It is not difficult to see that the time τ_1 of encounter of the sound wave front with the shock front is given by

$$\tau_1 = \frac{\tau_0 \beta_s \cos\phi}{\cos\phi - \beta_s}. \tag{72}$$

It is clear that the encounter is possible only if $\cos\phi > \beta_s$, as was also discussed for the first time in Ref. [23].

A natural question to ask is the following: Do the modes found in the previous sections actually hit the shock from behind once they are reflected or generated at the piston? If the piston is responsible for the appearance of the additional spectrum of eigenfrequencies, there should be some specific interaction between both surfaces. The task consists in evaluating the wave number vector $\vec{k}=(k_x,k_y)$ of each of the modes, in the resting fluid. In evaluating the angle it forms with the normal axis we will be able to decide whether that ray will actually hit the shock or not. It is convenient to use the results of Fraley [10], actually the mode amplitudes $a(s)$ and $b(s)$ shown in Eq. (62). We will analyze the values allowed to the projection k_x of $\vec{k}$ along the x axis of the SAE modes. The right facing sound ray, evaluated at any position $x<x_s$, has a Laplace amplitude given by [see Eq. (62) and the following discussion therein]

$$b(s_f)\exp(s_f\tau - kx\sqrt{s_f^2+1}). \tag{73}$$

We prefer to distinguish here between the Laplace variable used by Fraley (indicated by s_f) and ours (which we simply name s). It is clear that $|k_x|=k|\sqrt{s_f^2+1}|$. In addition, we can define q_f, such that $s_f=\sinh q_f$. Then, thanks to Eqs. (64) and (65), it is easy to get $s_f=\sinh(q-\theta_s)$, where $s=\sinh q$. Therefore, $\sqrt{s_f^2+1}=\cosh(q-\theta_s)$, and we obtain

$$k_{x/k} = -\cosh\theta_s\sqrt{s^2+1} + s\sin\theta_s = \sinh(-\alpha+\theta_s), \tag{74}$$

where use has been made of Eq. (32). We easily deduce, extrapolating from Eqs. (24) and (31), that the angle formed by the sound ray associated with the first acoustic emission mode with the horizontal axis is given by

$$\phi_0 = \arctan[1/\sinh(-\alpha_0+\theta_s)]. \tag{75}$$

The angle formed by the second shock mode is therefore given by

$$\phi_2 = \arctan[1/\sinh(-\alpha_0+3\theta_s)]. \tag{76}$$

Analogously, for the first piston mode, we get, extrapolating from Eq. (39),

$$\phi_1 = \arctan[1/\sinh(\alpha_0-2\theta_s)]. \tag{77}$$

A general formula for higher order modes is easy to deduce from the above results. It is interesting to see how these angles behave as a function of the incident shock Mach number for the SAE situations studied in this work. The study of the angles of reflection at the piston will allow us to understand which of the modes actually succeed in coupling the piston and the shock front. To this end, we plot in Fig. 11 the limiting angle given by $\arccos\beta_s$ [see Eq. (72) and the following discussion], and the angle of reflection of the first shock mode as given by Eq. (75). We have used the van der Waals gas studied in Fig. 3 (which corresponds to a dimensionless initial volume $Q_1=3$ and a dimensionless specific heat $\sigma_1=30$, as first studied in Ref. [7]). The horizontal axis is the incident shock Mach number and the curves start and end at those values between which there is acoustic emission at the shock front. We see that the angle of the sound ray lies outside the region of shock-piston influence, because the sound ray forms an angle ϕ_0 for which $\cos\phi_0 < \beta_s$. For this case, the shock emission mode does not interact with the shock after reflection at the piston and this mode satisfies the

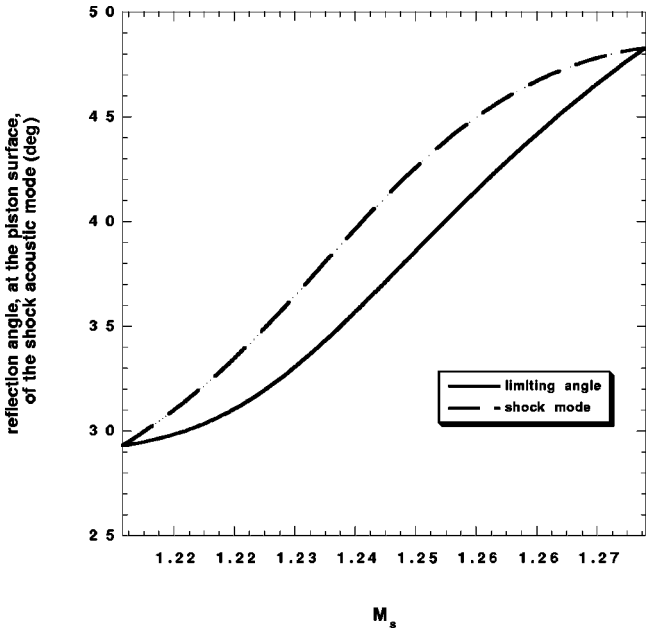

FIG. 11. Limiting angle curve and reflection angle of the first shock oscillation mode at the piston, for $\sigma_1=30$ and $Q_1=3$.

standard DK dispersion relationship, as expected. Let us change the gas parameter σ_1 and the initial volume Q_1 such that it is now possible to excite the first piston mode, but not the second shock mode. In Fig. 12 we show the angles of the rays associated with the first shock and piston modes, together with the corresponding limiting angle curve, for a van der Waals gas with $\sigma_1=30$ and $Q_1=25$. This case corresponds to stronger shocks than in the previous case. The minimum and maximum Mach numbers correspond to the zone of the space of parameters inside which it is possible to

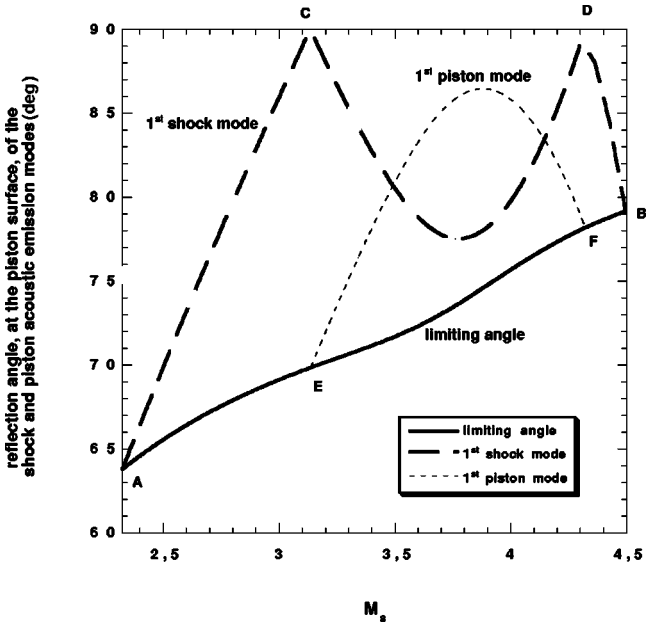

FIG. 12. Limiting angle curve, reflection angle of the first shock oscillation mode at the piston, and first piston mode, for $\sigma_1=30$ and $Q_1=25$.

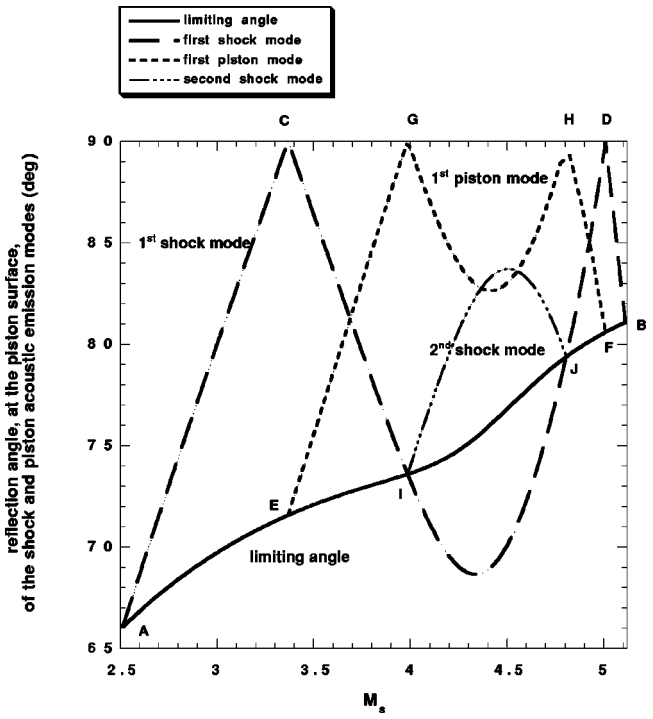

FIG. 13. Limiting angle curve, reflection angle of the first and second shock oscillation modes at the piston, and first piston mode, for $\sigma_1=80$ and $Q_1=35$.

excite the acoustic modes. Let us concentrate first on the curve representing ϕ_0 (the angle of the first shock mode ray). It starts increasing and soon reaches the value $\pi/2$ at the point *C*. Beyond that point, increasing the shock Mach number further makes the angle greater than 90°. This means that at that point the role played by the Fraley modes $a(s)$ and $b(s)$ is interchanged. That is, in the curved segment *CD*, it is the Fraley mode $a(s)$ which is now transporting the information from the piston to the shock. Anyway, independently of this detail, the discussion concerning the angle of interaction remains the same, as far as the coupling between both surfaces is concerned. The segment *CD* shows a minimum but the physical conditions are such that this minimum does not cross the limiting angle curve. Therefore, the first shock mode does not reach the shock from behind in this situation. The curve continues from *D* to the point *B* where it terminates. In between, at the point *E*, which has the same Mach number as the point *C*, the piston starts emitting its own mode. The angle ϕ_1 formed by this ray behaves in a similar way as ϕ_0 did in Fig. 11. It stays always above the limiting curve, which also means that this sound wave does not reach the shock front from behind. We now change the gas parameters to $\sigma_1=80$ and $Q_1=35$ and study the corresponding angles in Fig. 13. The limiting angle curve is the solid line *AB*. As before, we see that all the emission modes (either shock or piston modes) start and end on the limiting curve *AB*. Let us concentrate first, as before, on the curve associated with the first shock mode. It starts increasing at *A*, reaches the value $\pi/2$ at the point *C*, and starts decreasing. The behavior in the curved segment *CD* represents the role interchange between the $a(s)$ and $b(s)$ modes, as discussed

before. The points *C* and *E* have the same Mach number. Beyond the point *E*, the piston also starts emitting its own mode. The curve associated with the first shock mode decreases and goes below the limiting angle curve. This means that between the points *I* and *J* the piston succeeds in coupling piston and shock using the first shock mode. That is, between the points *I* and *J*, the shock interacts with the piston with its own first mode. We also see that, at the point *I*, the second shock mode is excited. The second mode angle curve increases and terminates at point *J*, where the first mode curve again crosses the limiting curve. Beyond the point *J*, there is no longer a second shock oscillation mode and the first shock mode does not interact with the shock any longer. This picture allows us to give a nice interpretation of the shock-piston coupling mechanism: the second shock mode is excited only when the first shock mode successfully arrives to the shock. It is expected that if there is a possibility of exciting a third shock mode, this will be because the second shock mode successfully arrives at the shock. We have been unable to get a third shock mode within the range of parameters used in this work. We have at hand a kind of iterative mechanism for the generation of the additional frequencies at the shock: the mode $n+1$ is excited only because the mode n has its rays inside the cone of influence defined by $\cos\phi=\beta_s$. Nested with the shock modes we will have the corresponding lower order piston modes. This happens, of course, in some well defined range of the initial parameters, as discussed in Eqs. (30) and (43). In this way, the role of the piston is crucial for the excitation of the additional modes found here. It is therefore clear that without a piston these additional oscillation modes will not be generated. This is the reason why the additional frequencies would never be predicted with an isolated shock model as has been used in the past 50 years.

D. Application of these results to the Richtmyer-Meshkov instability

In a real experiment, the shock will be driven by a contact surface separating two different fluids, which will never behave exactly as a rigid piston. As is known, when an incident planar shock strikes a corrugated surface that separates two fluids with different thermodynamic properties, the corrugation at the interface becomes unstable. The phenomenon, known as the Richtmyer-Meshkov instability (RMI) has been intensely studied for half a century, in particular in the inertial fusion community, where corrugated shocks are generated during the implosion of the thermonuclear target [10,12–18]. The outcome of the *incident shock-contact surface* interaction is a transmitted shock into the second fluid, and another shock or rarefaction is reflected back in the first fluid. The refracted fronts leave an initial circulation at both sides of the material interface, which will be later modified by the sonic interaction with the escaping fronts because of the acoustic field that fills the whole space. If both fluids are ideal gases, it is known that the shock front ripples decay to zero amplitude for large times. As a consequence, the normal and tangential velocities reach, in both gases, values asymptotically constant in time. For this to happen, each fluid will show a corresponding steady, rotational, and solenoidal velocity field. The fact that the sonic perturbations decay to zero when the fronts have traveled a distance several times the corrugation wavelength ensures the asymptotic incompressibility of the velocity field in both fluids, independently of the incident shock intensity [36]. This fact guarantees a constant asymptotic normal rate of growth of the contact surface ripple, a fundamental parameter that has been the subject of intensive research in the last five decades [10,12–18,36,37,39,40,42]. How would this picture change if one or both of the fluids exhibited spontaneous acoustic emission at the shocks? It is clear that an exact study of the effect of SAE on the RMI, for fluids with arbitrary equations of state, is well beyond the limits of this work. However, we could get a qualitative image of the changes introduced in the growth dynamics, on the basis of the conclusions that have been inferred in the preceding sections. As pointed out some lines above, the classical normal rate of growth of the interface in the RMI with ideal gases can be successfully calculated due to the asymptotic incompressibility of the velocity field, irrespective of the intensity of the incident shock. This is one of the ingredients that would be absent if one or both shock fronts started to emit acoustic waves downstream. The space would be filled with stable sound reverberations which do not decay to zero when $t\rightarrow\infty$, spoiling some of the mathematical simplifications that led to the simple growth rate formula found in Ref. [36]. It could be possible, but remains to be rigorously proved yet, that the asymptotic normal velocity in linear theory at the interface could be calculated now in the form $\delta v_i \sim \text{const}+f_{osc}(t)$. The term const would be calculated with a technique similar to that employed for ideal gases as has been done in Refs. [37,38], and $f_{osc}(t)$ would be that oscillating part that comes from the stable SAE modes filling the space at both sides of the material interface. It should be noted, however, that the function f_{osc} is likely to be different from zero only in those cases in which it is the piston that is radiating its own modes. That is, the effect of the shock SAE modes would not be directly seen as a stable, asymptotic oscillating contribution to the growth rate. Rather, the SAE modes of the shock would excite the SAE modes at the piston, and this last excitation is likely to contribute to the function f_{osc} commented on a few lines before. However, the shock SAE modes would enter into the const term, through the generation of vorticity [36,40]. In the ideal gas case, the vorticity profiles enter into the final growth rate calculation as a spatial average. The value of this average is important to get the exact growth rate in the strong compression situations [36,37,39,40]. In addition, in the ideal gas cases, the vorticity profile at either side of the contact surface is an oscillating function of space whose amplitude decreases asymptotically like $|x|^{-3/2}$. This fact provides us with a fast and highly accurate algorithm with which we can calculate the asymptotic normal growth with the desired precision. In the case of the SAE environment, the shock fronts will not generate a spatially decaying vorticity field away from the interface. On the contrary, the vorticity profiles in this case will oscillate with a constant amplitude. Therefore, the numerical value of the average of this spatial vorticity profile would be different as compared to the ideal gas case. This characteristic could also change

the iteration process with which we obtain the value of const. It is clear that these effects are a very interesting subejct of research which could certainly have a non-negligible impact in the field of high energy density experiments in fluids with more exotic equations of state. This task is left for future work.

VI. CONCLUSIONS

To summarize the work presented here, we briefly review the results obtained and make some further comments. The exact solution to the wave equation in the space between a corrugated piston and the corrugated shock was calculated when $h<1-2\beta_s^2$. The conditions under which such a solution exhibits modes of stable oscillation have been discussed. It is seen that, in addition to the well known DK mode of acoustic emission, the shock could also exhibit other (finite in number) stable eigenmodes. All these modes are excited simultaneously at $t=0^+$. The standard DK criterion [Eq. (2)] has been modified to account for these additional modes, as shown in Eq. (30). Later on, when the normal and transverse waves decay, the eigenfunctions will be the only perturbations evolving stably on the shock surface. As the shock propagates, the waves emitted into the compressed fluid fill the space up to the piston surface, and if analogous conditions are satisfied at the piston surface [Eq. (43)], the pressure perturbations at the piston will also exhibit stable oscillations. The same could be said for any other mathematical surface traveling at constant speed, that is, $0<\theta<\theta_s$. Situations in which these results can be verified, at least theoretically, have been presented by studying a van der Waals equation of state. Other works that have studied the same subject have been compared with ours and the reasons for agreement and/or disagreement have been discussed. It has also been shown that the piston surface plays a prominent role in the excitation of the additional shock oscillation modes found here. Normally, from all the waves reflected at the piston, only a small portion reaches the shock from behind. In general, the first shock oscillation mode does not arrive at the shock after reflection at the contact surface. However, for some substances, at high enough compressions, this mode can actually enter into the cone of influence between shock and piston. In this way, the first shock mode successfully arrives at the shock surface, which in turn excites the second mode. It is therefore seen, that thanks to successful reflection at the piston, the second mode is generated by the interaction of the shock with its own first mode. In a similar way, it is expected that in some other regions of the space of parameters, and at higher compressions, this second mode would excite a third shock mode, after adequate reflection at the piston, and so on. Nested in this process of shock mode generation, we will also see a similar excitation pattern for the SAE modes at the piston.

ACKNOWLEDGMENTS

This work was supported by Grant No. PAI-02-002 of Junta de Castilla–La Mancha, Consejera de Ciencias y Tecnologicas, and Grant No. FTN 2003-00721 of Ministry of Science and Technology. Stimulating discussions with and encouragement from K. Nishihara, R. Piriz, and S. Abarzhi are gratefully acknowledged.

APPENDIX: MODE AMPLITUDES

The amplitude a_0 of the standard DK mode is $a_0=f_0K_0/w_0$, where $f_0=f^0_{aux}(iw_0)$, $K_0=K(0)(iw_0)$, and

$$f^{(0)}_{aux}(q)\equiv\alpha_2(q)+\alpha_2(q+2\theta_s)+[\cosh(q+2\theta_s)+\alpha_1(q+2\theta_s)]\delta P_s(q+2\theta_s), \tag{A1}$$

$$K^{(0)}(q)\equiv\frac{w^4-1}{1-\alpha_{10}w(w^2+\zeta_0^2)}. \tag{A2}$$

The amplitude of the piston mode is $a_1=f_1K_1/w_1$, where $f_1=f^{(1)}_{aux}(iw_1)$, $K_1=K^{(1)}(iw_1)$. The functions $f^{(1)}_{aux}$ and K_1 are defined by

$$f^{(1)}_{aux}(w)\equiv\frac{4\delta v_0w(w^2e^{2\theta_s}+1)}{w^2e^{2\theta_s}-1}+\frac{e^{\theta_s}(w^2e^{4\theta_s}+1)[(1+\alpha_{10})w^4+(4\alpha_{11}-2\alpha_{10})e^{-2\theta_s}w^2-(1-\alpha_{10})e^{-4\theta_s}]\delta P_i(e^{2\theta_s}w)}{w(w^2e^{2\theta_s}-1)}, \tag{A3}$$

$$K^1(w)=\frac{e^{-3\theta_s}(w^2e^{2\theta_s}-1)}{(1-\alpha_{10})w(w^2+\zeta_1^2)}, \tag{A4}$$

and $\zeta_1=\sqrt{U_0}e^{-\theta_s}$. The amplitude of the second shock mode is given by $a_2=f_2K_2/w_2$, where $f_2=f^{(2)}_{aux}(iw_2)$, $K_2=K^{(2)}(iw_2)$, and

$$f^{(2)(q)}_{aux}\equiv\lambda_2(q)[\alpha_2(q+2\theta_s)+\alpha_2(q+4\theta_s)]+\lambda_2(q)[\cosh(q+4\theta_s)+\alpha_1(q+4\theta_s)]\delta P_s(q+4\theta_s), \tag{A5}$$

$$K^{(2)}=\frac{e^{-6\theta_s}(w^2e^{4\theta_s}-1)(w^2+1)}{1-\alpha_{10}w(w^2+\zeta_2^2)}. \tag{A6}$$

[1] L. D. Landau, *Fluid Mechanics* (Butterworth-Heinemann, Oxford, 1995).
[2] Ya. B. Zeldovich and Yu. P. Raizer, *Physics of Shock Waves and High Temperature Hydrodynamic Phenomena* (Dover, Mineola, NY, 2002).
[3] G. E. Duvall and R. A. Graham, Rev. Mod. Phys. **49**, 523 (1977).
[4] E. T. Vishniac, Astrophys. J. **274**, 152 (1983).
[5] G. H. Miller and T. J. Ahrens, Rev. Mod. Phys. **63**, 919 (1991).
[6] J. W. Bates and D. C. Montgomery, Phys. Fluids **11**, 463 (1999).
[7] J. W. Bates and D. C. Montgomery, Phys. Rev. Lett. **84**, 1180 (2000).
[8] R. Ishizaki and K. Nishihara, Phys. Rev. Lett. **78**, 1920 (1997).
[9] A. L. Velikovich, J. P. Dahlburg, A. J. Schmitt, J. H. Gardner, L. P. Phillips, F. L. Cochran, Y. K. Chong, G. Dimonte, and N. Metzler, Phys. Plasmas **7**, 1662 (2000).
[10] G. Fraley, Phys. Fluids **29**, 376 (1986).
[11] J. Lindl, Phys. Plasmas **2**, 3933 (1995).
[12] R. D. Richtmyer, Commun. Pure Appl. Math. **13**, 297 (1960).
[13] E. E. Meshkov, Fluid Dyn. **4**, 101 (1969).
[14] A. L. Velikovich, A. Schmitt, J. H. Gardner, and N. Metzler, Phys. Plasmas **8**, 592 (2001).
[15] S. G. Glendinning, J. Bolstad, D. G. Braun, M. J. Edwards, W. W. Hsing, B. F. Lasinski, H. Louis, A. Milles, J. Moreno, T. A. Peyser, B. A. Remington, H. F. Robey, E. J. Turano, C. P. Verdon, and Y. Zhou, Phys. Plasmas **10**, 1931 (2003).
[16] H. Azechi, M. Nakai, K. Shigemori, N. Miyanaga, H. Shiraga, H. Nishimura, M. Honda, R. Ishizaki, J. G. Wouchuk, H. Takabe, K. Nishihara, K. Mima, A. Nishiguchi, and T. Endo, Phys. Plasmas **4**, 4079 (1997).
[17] T. R. Dittrich, S. W. Haan, M. M. Marinak, S. M. Pollaine, D. E. Hinkel, D. H. Munro, C. P. Verdon, G. L. Strobel, R. McEachern, R. C. Cook, C. C. Roberts, D. C. Wilson, P. A. Bradley, L. R. Foreman, and W. S. Varnum, Phys. Plasmas **6**, 2164 (1999).
[18] R. L. Holmes *et al.*, J. Fluid Mech. **389**, 55 (1999).
[19] A. R. Piriz, Phys. Plasmas **8**, 997 (2001).
[20] A. E. Roberts, Los Alamos Scientific Laboratory Report No. LA-299, 1945 (unpublished).
[21] S. P. D'yakov, Zh. Eksp. Teor. Fiz. **27**, 288 (1954).
[22] V. M. Kontorovich, Sov. Phys. JETP **6**, 1179 (1957).
[23] V. M. Kontorovich, Akust. Zh. **5**, 314 (1959).
[24] J. J. Erpenbeck, Phys. Fluids **5**, 604 (1962).
[25] G. R. Fowles and G. W. Swan, Phys. Rev. Lett. **30**, 1023 (1973).
[26] G. W. Swan and G. R. Fowles, Phys. Fluids **18**, 28 (1975).
[27] G. R. Fowles, Phys. Fluids **18**, 76 (1975).
[28] G. R. Fowles, Phys. Fluids **24**, 220 (1981).
[29] I. Rutkevich, E. Zaretsky, and M. Mond, J. Appl. Phys. **81**, 7228 (1997).
[30] M. Mond and I. M. Rutkevich, J. Fluid Mech. **275**, 121 (1994).
[31] M. Mond and I. M. Rutkevich, Phys. Fluids **14**, 1468 (2002).
[32] M. Mond and L. O'C. Drury, Astron. Astrophys. **332**, 385 (1998).
[33] J.-Ch. Robinet, J. Gressier, G. Casalis, and J.-M. Moschetta, J. Fluid Mech. **417**, 237 (2000).
[34] R. M. Zaidel', J. Appl. Math. Mech. **24**, 316 (1958).
[35] M. G. Briscoe and A. A. Kovitz, J. Fluid Mech. **31**, 529 (1968).
[36] J. G. Wouchuk and K. Nishihara, Phys. Plasmas **4**, 1028 (1997).
[37] J. G. Wouchuk, Phys. Rev. E **63**, 056303 (2001).
[38] J. G. Wouchuk, Phys. Plasmas **8**, 2890 (2001).
[39] J. G. Wouchuk and K. Nishihara, Phys. Plasmas **3**, 3761 (1996).
[40] I. S. Gradshteyn and I. M. Ryzshik, *Table of Integrals, Series, and Products*, corrected and enlarged ed. (Academic, New York, 1980).
[41] A. L. Velikovich, Phys. Fluids **8**, 1666 (1996).
[42] L. M. Milne-Thomson, *The Calculus of Finite Differences* (Macmillan, London, 1933), Chap. 8.
[43] T. L. Saaty, *Modern Non Linear Equations* (Dover, New York, 1981), p. 164.
[44] P. A. Thompson, Phys. Fluids **14**, 1843 (1971).
[45] N. C. Freeman, Proc. R. Soc. London, Ser. A **228**, 341 (1955).
[46] W. R. LePage, *Complex Variables and the Laplace Transform for Engineers* (Dover, New York, 1980).
[47] J. W. Bates, Phys. Rev. E **69**, 056313 (2004).
[48] D. Munro, Phys. Fluids B **1**, 134 (1989).
[49] R. Courant and D. Hilbert, *Methods of Mathematical Physics* (Wiley, New York, 1953), Vols. I and II.
[50] J. D. Jackson, *Classical Electrodynamics* (Wiley, New York, 1999).
[51] H. F. Weinberger, *Partial Differential Equations* (Blaisdell, New York, 1965).